The Design of Selective Chelating Agents: 1,3,5-Trideoxy-1,3,5-tris-(dimethylamino)-*cis*-inositol, a Powerful Ligand for Hard and Highly Charged Metal Ions**

Kaspar Hegetschweiler,* Thomas Kradolfer, Volker Gramlich, and Robert D. Hancock

Abstract: A series of compounds containing the mononuclear complexes $[M(tdci)_2]^{3+}$ (tdci = 1,3,5-trideoxy-1,3,5-tris(dimethylamino)-*cis*-inositol, M = Al, Fe, Ga, In) and $[M(tdci)_2]^{4+}$ (M = Ti, Ge, Sn) was prepared and characterized by elemental analysis, NMR spectroscopy, and FAB mass spectrometry. Characteristic fragmentation reactions in the mass spectra were elucidated. X-ray analysis of the Al^{III}, Fe^{III}, Ga^{III}, and In^{III} complexes revealed that two neutral, zwitterionic tdci ligands coordinate to the metal cation exclusively through deprotonated alkoxo groups. The six coordinated oxygen donors and the six N–H protons form a hydrophilic pocket, whereas the two cyclohexane rings and the twelve methyl groups form two hydrophobic shells. The hydrophilic pocket is filled with twelve water molecules, which are arranged as a second and a third coordination sphere around the metal cation. The reactivity in aqueous solution was investigated by potentiometric measurements. The bis complexes proved to be stable at pH 7. The evaluated formation constants show an increase of stability in the order $Al^{III} < In^{III} < Ga^{III} < Fe^{III}$. The measurements established that tdci is one of the most effective tridentate ligands for small ($r \leq 0.8$ Å) and highly charged cations. The different chelating properties of tdci and of the unmethylated 1,3,5-triamino-1,3,5-trideoxy-*cis*-inositol are discussed in terms of different steric requirements and different types of solvation of the corresponding complexes in aqueous solution.

Keywords
chelate ligands · hydrogen bonds · ligand design · mass spectrometry · stability constants

Introduction

In the previous contributions of this series, we reported the remarkable metal-binding properties of 1,3,5-triamino-1,3,5-trideoxy-*cis*-inositol (taci).[1–7] This versatile ligand readily forms complexes with divalent, trivalent, or even tetravalent metal ions in aqueous solution. The high versatility is based on the availability of the N_3, N_2O, NO_2, and O_3 coordination modes (Scheme 1, (i)–(iv)) and on the ability to coordinate in different tautomeric forms. The ligand can thus provide either hydroxyl or alkoxo groups for metal binding (e.g., Scheme 1, (ivA) and (ivB)).

The binding properties of taci can easily be modified by introducing suitable substituents at the oxygen or nitrogen donor atoms. Two different types of substituents are conceivable: a) substituents that carry additional donor atoms and thus yield a more extended and versatile ligand, and b) substituents without any additional donor atoms, which disable some of the binding modes for steric reasons and thus provide a less versatile but more selective ligand. In three preliminary papers, we provided examples for both types of ligand: Reaction of taci with salicylic aldehyde followed by hydrogenation of the condensation product yielded the potentially hexadentate 1,3,5-tride-

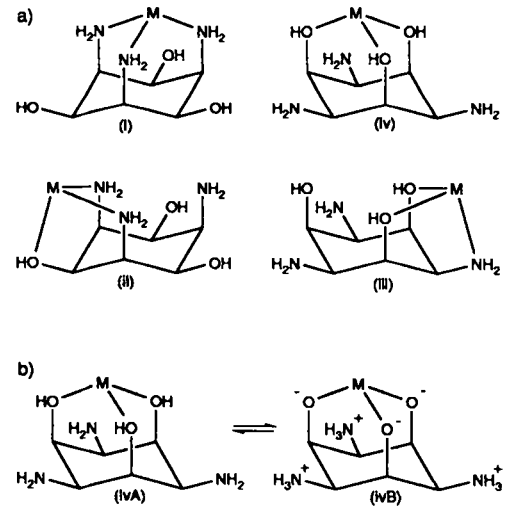

Scheme 1. Coordination modes available to taci.

[*] Dr. K. Hegetschweiler, Dr. T. Kradolfer
Laboratorium für Anorganische Chemie, ETH-Zentrum
CH-8092 Zürich (Switzerland)
Telefax: Int. code + (1)632-1090
Dr. V. Gramlich
Institut für Kristallographie und Petrographie, ETH Zentrum
Prof. R. D. Hancock
Centre for Molecular Design, Department of Chemistry
University of the Witwatersrand, WITS 2050, Johannesburg (South Africa)

[**] 1,3,5-Triamino-1,3,5-trideoxy-*cis*-inositol, a Ligand with a Remarkable Versatility for Metal Ions, Part 7. Part 6: K. Hegetschweiler, M. Ghisletta, T. F. Fässler, R. Nesper, *Angew. Chem. Int. Ed. Engl.* **1993**, *32*, 1426.

0570-0833/95/0101-0074 $ 10.00+.25/0

oxy-1,3,5-tris(2-hydroxybenzylamino)-*cis*-inositol (H_3thci),[8] whereas simple methylation of the amino groups resulted in the formation of 1,3,5-trideoxy-1,3,5-tris(dimethylamino)-*cis*-inositol (tdci).[9, 10] Here, the bulky $(CH_3)_2N$ groups impede chair conversion and the coordination modes (i) and (ii) (Scheme 1) are therefore disabled. Complete methylation of the amino groups finally yielded a ligand in which only site (iv) (Scheme 2) is available for metal binding.[10]

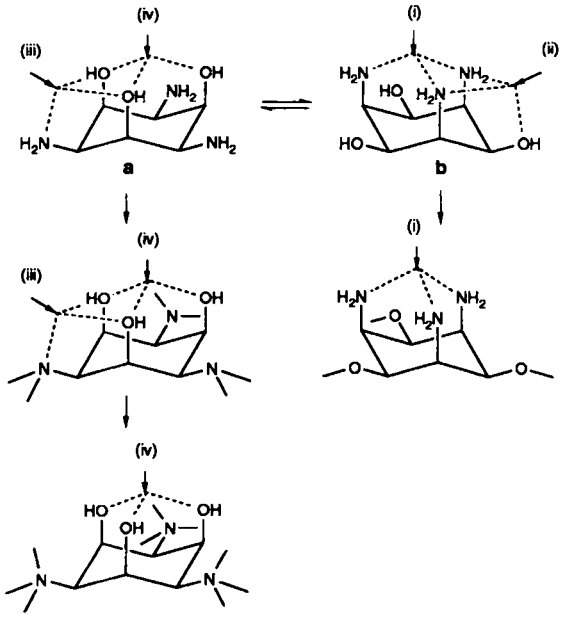

Scheme 2. Effect of substituents on the availability of binding sites in taci.

Owing to the selective blocking of site (i) and site (ii), tdci interacts preferably with oxophilic (i.e., hard) metal ions. This preference is clearly expressed in the high stability of $[Fe(tdci)_2]^{3+}$ and $[Al(tdci)_2]^{3+}$ on the one hand, and by rather weak interactions of tdci with Cu^{II} on the other.[9] Hence, selective alkylation of taci opens new routes for the design of novel, highly specific chelators as required, for instance, in medicine for the removal of Fe^{III} or Al^{III}.[11] In this context, it is particularly noteworthy that $[Al(tdci)_2]^{3+}$ is even more stable than the parent complex $[Al(taci)_2]^{3+}$, although the two complexes have a similar AlO_6 coordination sphere. The surprisingly high difference in their stability ($\Delta \log \beta_2 \approx 10^8$) is thus a consequence of rather small and peripheral alterations in the molecular structure of the ligand. To get a better understanding of this unexpected effect, we performed a comprehensive, comparative investigation of the coordination chemistry of taci and tdci. In the present contribution, we report the preparation and characterization of the bis complexes $[M(tdci)_2]^{z+}$ ($M = Al^{III}$, Ga^{III}, Fe^{III}, In^{III}, Si^{IV}, Ti^{IV}, Ge^{IV}, Sn^{IV}), as well as their stability and reactivity in aqueous solution. In addition, the X-ray structures of the Al, Fe, Ga, and In complexes will be presented. Molecular mechanics calculations provide a systematic elucidation of steric effects in these complexes. The prerequisites for a successful design of effective chelators of the taci type are also discussed.

Experimental Section

Spectroscopy, Mass Spectrometry, and Analyses: The ^{1}H NMR and ^{13}C NMR spectra were measured on a Bruker AC200 spectrometer at 200.13 and 50.38 MHz, respectively. Chemical shifts are given relative to sodium [D_4](trimethylsilyl)propionate as internal standard. ^{27}Al NMR were recorded on a Bruker AC250 spectrometer at 65.177 MHz. A solution of 0.1 M $Al(NO_3)_3$ in D_2O was used as external standard. Stock solutions of the complexes were made up in D_2O. The pD was then adjusted by adding appropriate amounts of NaOD to 0.4 mL of the stock solutions. Additional D_2O was added to get a final volume of 0.6 mL, and $-\log[D^+]$ (= pH + 0.4) was checked with a glass electrode, which was calibrated with aqueous buffer solutions.

FAB^+ mass spectra were measured on a VG ZAB VSEQ instrument. Test solutions were prepared by dissolving the samples in water and mixing the resulting solutions with a glycerol matrix prior to introduction in the spectrometer. The natural abundance, given in ref. [12], was used to calculate the amount of the different isotopomers of an ion. Ion overlap was analyzed by least squares calculation [13]; $\sum(I_{calcd} - I_{obs})^2$ = min. IR spectra (KBr wafer) were recorded on a Perkin-Elmer 883 infrared spectrophotometer. C, H, N analyses were performed by D. Manser, Laboratorium für Organische Chemie, ETH Zürich. Cl content was determined by potentiometric titration with standardized $AgNO_3$ as titrant.

Materials: Tdci was prepared according to ref. [10]. $GaCl_3$ (anhydrous), $In(NO_3)_3 \cdot H_2O$, $InCl_3$ (anhydrous), $Tl(NO_3)_3 \cdot 3H_2O$, $SiCl_4$, $TiCl_4$, $GeCl_4$, and $SnCl_4$ were commercially available products of reagent grade quality. They were used without further purification. MeOH was dried according to ref. [14].

Preparation of the Complexes: $[Al(tdci)_2]Cl_3 \cdot 14.5H_2O$ (**1**) and $[Fe(tdci)_2]Cl_3 \cdot 14.5H_2O$ (**2**) were prepared as described previously [9].

$[Ga(tdci)_2]Cl_3 \cdot 14.5H_2O$ (3): A solution of $GaCl_3$ (0.3 g, 1.7 mmol) in MeOH (3.5 g) was added to a solution of tdci (0.91 g, 3.5 mmol) in MeOH (25 mL). Water (15 mL) was then added to the resulting clear solution. The solution was concentrated at 80 °C to a total volume of 15 mL and then cooled to room temperature. EtOH (45 mL) was added, and a white solid precipitated, which dissolved again by gentle heating. The solution was allowed to cool down slowly to room temperature. Colorless crystals, which proved to be suitable for single crystal X-ray analysis, were obtained. The crystals were dried in vacuo over P_2O_5, and the resulting solid was then allowed to stand in humid air until no further increase in weight was observed. Yield: 72%; $C_{24}H_{54}Cl_3GaN_6O_6 \cdot 14.5H_2O$ (960.0): calcd C 30.03, H 8.71, N 8.75; found C 30.25, H 8.60, N 8.70.

$[In(tdci)_2]Cl_3 \cdot 14.5H_2O$ (4a): A solution of $InCl_3$ (60 mg, 0.27 mmol) in MeOH (0.6 g) was added to a solution of tdci (150 mg, 0.57 mmol) in MeOH (3 mL). Water (3 mL) was then added to the resulting clear solution. The solution was concentrated at 80 °C to a total volume of 3 mL. After cooling to room temperature, the aqueous solution was layered with EtOH to yield single crystals suitable for X-ray analysis. The crystals were dried in vacuo over P_2O_5 and the resulting solid was then allowed to stand in humid air until no further increase in weight was observed. Yield: 65%; $C_{24}H_{54}N_6O_6Cl_3In \cdot 14.5H_2O$ (1005.1): calcd C 28.68, H 8.32, N 8.36; found C 28.67, H 7.90, N 8.31 [15].

$[In(tdci)_2]_{1-n}[H_{-1}In(tdci)_2]_n(NO_3)_{3-n} \cdot 13.5H_2O$ ($0 < n < 0.4$) (4b): A solution of $In(NO_3)_3 \cdot H_2O$ (0.6 g, 1.9 mmol) in MeOH (4.2 g) was added to a solution of tdci (1.0 g, 3.8 mmol) in MeOH (5 mL). Water (8 mL) was then added to the resulting clear solution. The solution was concentrated at 80 °C to a total volume of 8 mL and then cooled to room temperature. Acetone (30 mL) was added, and a white solid precipitated, which was filtered off, dried in vacuo over P_2O_5, and allowed to stand in humid air until no further increase in weight was observed. Yield: 70%. The extent of deprotonation (n) was poorly reproducible and was determined for each sample individually by acidimetric titration. However, the obtained value was always in excellent agreement with the elemental analyses of the complex. Example: $n = 0.22$, $C_{24}H_{53.78}N_{8.78}O_{14.34}In \cdot 13.5H_2O$: calcd C 27.38, H 7.73, N 11.68; found C 27.56, H 7.12, N 11.67 [15].

$[Si(tdci)_2]Cl_4 \cdot 10H_2O$ (5): A solution of $SiCl_4$ (47 mg, 0.28 mmol) in THF (2.4 g) was added slowly to a solution of tdci (152 mg, 0.58 mmol) in THF (10 mL). A white solid, which precipitated immediately during the addition, was filtered off, dried in vacuo over P_2O_5, and allowed to stand in humid air until no further increase in weight was observed. The yield was almost quantitative; $C_{24}H_{54}N_6O_6Cl_4Si \cdot 10H_2O$ (872.8): calcd C 33.03, H 8.55, N 9.63; found C 33.07, H 8.45, N 9.51.

$[Ti(tdci)_2]_{1-n}[H_{-1}Ti(tdci)_2]_nCl_{4-n} \cdot 14.5H_2O$ (6), $[Ge(tdci)_2]_{1-n}[H_{-1}Ge(tdci)_2]_n$-$Cl_{4-n} \cdot 14.5H_2O$ (7), and $[Sn(tdci)_2]Cl_4 \cdot 13.5H_2O$ (8): A solution of MCl_4 (1.7 mmol) in MeOH (3.9 g) was added to a solution of tdci (890 mg, 3.41 mmol) in MeOH (20 mL). Water (15 mL) was then added, and the solution was concentrated at 80 °C to a total volume of 15 mL. After the solution had cooled to room temperature, acetone (60 mL) was added. The solution was allowed to stand at 4 °C for 24 h. A colorless product crystallized, which was filtered off, dried in vacuo over P_2O_5 and allowed to equilibrate in humid air until no further increase in weight was observed. The amount of deprotonation (n) was determined by acidimertric titration. **6**: 78% yield, $C_{24}H_{53.3}N_6O_6Cl_{3.3}Ti \cdot 14.5H_2O$ ($n = 0.7$): calcd C 30.40, H 8.75, N 8.86, Cl 12.34; found C 30.47, H 8.35, N 8.86, Cl 12.20 [15]. **7**: 84% yield, $C_{24}H_{53.76}N_6O_6Cl_{3.76}Ge \cdot 14.5H_2O$ ($n = 0.24$): calcd C 29.13, H 8.43, N 8.49, Cl 13.47; found C 29.25, H 8.13, N 8.42, Cl 13.46 [15]. **8**: 80% yield, $C_{24}H_{54}N_6O_6Cl_4Sn \cdot 13.5H_2O$ (1026.4): calcd C 28.08, H 7.95, N 8.19, Cl 13.82; found C 28.16, H 7.56, N 8.12, Cl 13.80 [15].

  0570-0833/95/0101-0075 $ 10.00+.25/0

Table 1. Crystallographic data for the compounds $[M(tdci)_2]Cl_3 \cdot 15H_2O$ (**1**, **2**, **3**, and **4a**).

	Al (**1**)	Fe (**2**)	Ga (**3**)	In (**4a**)
chem. formula	$C_{24}H_{84}AlCl_3N_6O_{21}$	$C_{24}H_{84}Cl_3FeN_6O_{21}$	$C_{24}H_{84}Cl_3GaN_6O_{21}$	$C_{24}H_{84}Cl_3InN_6O_{21}$
fw	926.3	955.2	969.0	1014.1
cryst. size/mm	0.2 × 0.2 × 0.2	0.3 × 0.3 × 0.3	0.3 × 0.3 × 0.3	0.3 × 0.2 × 0.1
space group	$R\bar{3}$ (no. 148)	$R\bar{3}$ (no. 148)	$R\bar{3}$ (no. 148)	$R\bar{3}$ (no. 148)
cryst. syst.	trigonal	trigonal	trigonal	trigonal
a/Å	17.37(1)	17.39(2)	17.411(2)	17.407(2)
c/Å	12.96(1)	13.05(1)	12.980(3)	13.188(3)
V/Å^3	3388(5)	3419(7)	3408(1)	3461(1)
Z	3	3	3	3
T/K	293	293	293	293
$\lambda(Mo_{K\alpha})$/Å	0.71073	0.71073	0.71073	0.71073
ρ_{calcd}/g cm^{-1}	1.362	1.392	1.417	1.460
μ/cm^{-1}	3.000	5.84	8.59	7.62
trans. coeff.			0.7401/0.7863	0.8081/0.9104
$2\theta_{max}$/°	45	45	50	45
measured refl.	985	993	2660	1006
unique refl.	985	993	1333 (R_{int} = 4.15%)	1006
obs. refl., $I > 2\sigma(I)$	837	811	1256	965
no. of parameters	137	137	84	84
$R(F_o)$/% [a]	4.57	4.06	5.28	4.59
$Rw(F_o)$/% [b]	5.92	4.66	7.67	6.74

[a] $R = \sum||F_o| - |F_c||/\sum|F_o|$. [b] $R_w = [\sum w(|F_o| - |F_c|)^2/\sum w|F_o|^2]^{1/2}$, $w = 1/\sigma^2(|F_o|)$.

X-ray Diffraction Studies: Data collection for **1**, **2**, **3**, and **4a** was performed on a four-circle Picker-Stoe diffractometer with graphite-monochromatized $Mo_{K\alpha}$ radiation. Crystallographic data are summarized in Table 1. One standard reflection was checked every 120 reflections, however, no decrease of intensity was noted. The data were corrected for Lorentz and polarization effects. A face-indexed numerical absorption correction was applied for the Ga and the In complex. The four compounds all crystallize in the space group $R\bar{3}$ and are isomorphous. The structure was solved by direct methods of SHELXTL-PLUS (VMS) [16]. All non-hydrogen atoms of the $[M(tdci)_2]^{3+}$ molecules were easily located in the difference Fourier map. Three additional peaks in the asymmetric unit indicated the positions of the three Cl^- counter ions and of twelve water molecules. The most intense peak was assigned to the position of Cl^-. Since the molecular formula requires only three counterions, an occupancy factor of 0.5 was used initially. However, it seems highly probable that three Cl^- ions and three water molecules occupy this position at random. This assumption is supported by a significant decrease of the R factor when the occupancy factor is increased from 0.5 to 0.75, and also by elemental analyses, which indicated the presence of 14–15 equiv of water per equiv of complex. Anisotropic displacement parameters were used for all non-hydrogen atoms in the final full-matrix least-squares calculations. The positions of the hydrogen atoms of the $[M(tdci)_2 \cdot 12H_2O]^{3+}$ entities could be localized in the difference Fourier map. For the Al and Fe complex, they were refined with variable isotropic displacement parameters. For the Ga and the In complex, they were included in the refinement as fixed values with isotropic displacement parameters of 0.05 Å^2 and not refined. The hydrogen atomic positions for the remaining three water molecules were not considered. Atomic coordinates are given in Table 2, bond lengths and selected bond angles in Tables 3 and 4, respectively.

Molecular Mechanics: Calculations were carried out with the SYBYL program [17]. The scans of strain energy as a function of metal ion radius were carried out as described previously [18], except that a value of 125° was used for a strain-free M-O-C angle. Recently, Hay et al. suggested that oxygen donors have a nearly trigonal-planar rather than tetrahedral mode of coordination to many metal ions [19]. This suggestion is in agreement with our observation of an M-O-C angle of about 120° in taci and tdci complexes with a low-strain type(iv) structure (Scheme 1). Therefore, in contrast to ref. [6] and [18], the value of Hay et al. has been used here. However, the positions of the minima in the

Table 2. Atomic coordinates and equivalent isotropic displacement parameters with estimated standard deviations in parentheses for non-hydrogen atoms of $[M(tdci)_2]Cl_3 \cdot 15H_2O$ (**1**, **2**, **3**, **4a**; M = Al, Fe, Ga, In).

atom	x	y	z	U_{eq}/Å^2 [a]	atom	x	y	z	U_{eq}/Å^2 [a]
		$[Al(tdci)_2]Cl_3 \cdot 15H_2O$ (**1**)					$[Ga(tdci)_2]Cl_3 \cdot 15H_2O$ (**3**)		
Al	0	0	0	0.022(1)	Ga	0	0	0	0.021(1)
Cl [b, c]	0.1794(1)	0.1668(1)	0.4826(1)	0.088(1)	Cl [b, c]	0.1795(2)	0.1665(2)	0.4835(2)	0.089(1)
O [c]	0.0995(1)	0.0717(1)	0.0861(1)	0.026(1)	O [c]	0.1026(2)	0.0741(2)	0.0894(2)	0.027(1)
N [c]	0.1333(2)	−0.0511(2)	0.1980(2)	0.030(1)	N [c]	0.1328(3)	−0.0516(2)	0.1999(3)	0.031(2)
C(1) [c]	0.0662(2)	−0.0257(2)	0.2341(2)	0.027(1)	C(1) [c]	0.0665(3)	−0.0263(3)	0.2358(3)	0.028(2)
C(2) [c]	0.0935(2)	0.0677(2)	0.1938(2)	0.026(1)	C(2) [c]	0.0944(3)	0.0685(3)	0.1968(3)	0.026(2)
C(11) [c]	0.2256(2)	0.0111(3)	0.2376(3)	0.047(2)	C(11) [c]	0.2257(3)	0.0108(4)	0.2392(4)	0.049(2)
C(12) [c]	0.1081(3)	−0.1443(2)	0.2263(3)	0.044(2)	C(12) [c]	0.1079(3)	−0.1435(3)	0.2284(4)	0.045(2)
O(1w) [c]	0.2463(2)	0.1861(2)	0.0027(2)	0.043(1)	O(1w) [c]	0.2485(2)	0.1855(2)	0.0020(2)	0.042(1)
O(2w) [c]	0.2474(2)	0.3474(2)	−0.0181(2)	0.062(1)	O(2w) [c]	0.2485(3)	0.3478(3)	−0.0154(3)	0.060(2)
		$[Fe(tdci)_2]Cl_3 \cdot 15H_2O$ (**2**)					$[In(tdci)_2]Cl_3 \cdot 15H_2O$ (**4a**)		
Fe	0	0	0	0.019(1)	In	0	0	0	0.021(1)
Cl [b,c]	0.1794(1)	0.1685(1)	0.4847(1)	0.083(1)	Cl [b, c]	0.1703(2)	0.1791(2)	0.5144(2)	0.085(2)
O [c]	0.1033(1)	0.0743(1)	0.0929(2)	0.023(1)	O [c]	0.1088(2)	0.0304(2)	0.0993(3)	0.025(2)
N [c]	0.1330(2)	−0.0510(2)	0.2008(2)	0.027(1)	N [c]	0.0511(3)	−0.1327(3)	0.2027(3)	0.028(2)
C(1) [c]	0.0662(2)	−0.0258(2)	0.2372(3)	0.024(2)	C(1) [c]	0.0257(3)	−0.0669(3)	0.2419(4)	0.026(2)
C(2) [c]	0.0942(2)	0.0682(2)	0.1997(2)	0.022(2)	C(2) [c]	0.0956(3)	0.0265(3)	0.2047(4)	0.026(2)
C(11) [c]	0.2255(3)	0.0111(3)	0.2366(3)	0.043(2)	C(11) [c]	0.1445(4)	−0.1084(4)	0.2311(5)	0.044(3)
C(12) [c]	0.1086(3)	−0.1440(3)	0.2277(3)	0.041(2)	C(12) [c]	−0.0114(4)	−0.2262(4)	0.2382(5)	0.046(3)
O(1w) [c]	0.2482(2)	0.1859(2)	0.0000(2)	0.040(1)	O(1w) [c]	0.1851(3)	0.2488(3)	0.0032(3)	0.040(2)
O(2w) [c]	0.2484(2)	0.3473(2)	−0.0156(3)	0.059(2)	O(2w) [c]	0.2499(3)	−0.0971(3)	−0.0119(4)	0.059(3)

[a] $U_{eq} = {}^1/_3\sum_i\sum_j U_{ij}a_i^*a_j^*\mathbf{a}_i\mathbf{a}_j$. [b] Occupancy factor = 0.75 (see text). [c] Symmetry operators: $-x, -y, -z$; $-y, x-y, z$; $y, -x+y, -z$; $-x+y, -x, z$; $x-y, x, -z$.

0570-0833/95/0101-0076 $ 10.00+.25/0 Chem. Eur. J. 1995, 1, No. 1

Table 3. Bond lengths [Å] of the $[M(tdci)_2]^{3+}$ complexes **1**, **2**, **3**, and **4a** with estimated standard deviations in parentheses.

bond	Al (**1**)	Fe (**2**)	Ga (**3**)	In (**4a**)
M–O	1.906(2)	2.011(3)	1.974(2)	2.141(4)
O–C(2)	1.400(3)	1.401(4)	1.399(4)	1.404(6)
N–C(1)	1.513(5)	1.510(6)	1.502(8)	1.510(9)
N–C(11)	1.506(5)	1.495(5)	1.516(6)	1.508(8)
N–C(12)	1.497(5)	1.494(6)	1.481(7)	1.510(7)
C(1)–C(2)	1.536(4)	1.534(6)	1.554(7)	1.545(6)
C(1)–C(2A)	1.528 (5)	1.522(7)	1.531(8)	1.545(10)

Table 4. Selected bond angles [°] of the $[M(tdci)_2]^{3+}$ complexes **1**, **2**, **3**, and **4a** with estimated standard deviations in parentheses.

angle	Al (**1**)	Fe (**2**)	Ga (**3**)	In (**4a**)
O-M-O [a]	89.2(1)	87.4(1)	88.9(1)	86.5(1)
O-M-O' [b]	90.8(1)	92.6(1)	91.1(1)	93.5(1)
C-O-M	122.1(1)	121.3(2)	120.9(2)	119.3(3)

[a] Intraligand. [b] Interligand, see ref. [26].

plots of $\sum U$ versus r_M (Fig. 9) do not change significantly when 125° is used rather than 109°.

Potentiometric Measurements: All potentiometric titrations were carried out at 25 °C, with an Orion 720A pH/mV meter, a Phillips GAH 420 glass electrode, and an Ag/AgCl reference electrode, fitted with a salt bridge containing 0.1, 0.2, 0.5, or 1.0 M KNO_3 or KCl. The sample solutions were titrated with 0.1, 0.2, 0.5, or 1.0 M KOH; 0.1 M HNO_3; or 0.1 M HCl, dispensed from a Metrohm 665 piston burette. The ionic strength was adjusted by adding appropriate amounts of KNO_3 or KCl to the test solutions. The potential measurements for the continuous titrations were performed as described previously [2,4,6,9]. In the batch titrations of **1**, **2**, and **7**, appropriate amounts of 0.1 M HCl were added to 22 individually sealed and thermostated sample solutions. An equilibration time of 72 h was allowed [9]. Further experimental details are summarized in Tables 5–7. The titration curves and species distribution plots are shown in Figures 1 and 2.

Table 5. Potentiometric data (25 °C, 0.1 mol dm^{-3} KCl) and evaluated equilibrium constants for the acidimetric titrations of **1** and **3** (estimated standard deviations in parentheses) [43].

metal (compound)	Al (**1**)	Al (**1**)	Al (**1**)	Ga (**3**)
titrant/mol dm^{-3}	HCl, 0.05 [a]	HCl, 0.1	HCl, 0.1	HCl, 0.1
$[M]_t$/mol dm^{-3}	5×10^{-4}	10^{-3}	2×10^{-3}	10^{-3}
$[tdci]_t$/mol dm^{-3}	10^{-3}	2×10^{-3}	4×10^{-3}	2×10^{-3}
type of titration	batch	batch	batch	continuous
evaluated range [b]	0.08–2.96	0.15–3.00	0.08–2.96	0.05–2.72
no. of data points	22	20	22	60
meas. time per point/h	72	72	72	0.25
$\log\beta(ML_xH_y)$ [c]				
x y	hydrolysis products [d]			
0 −1	−5.3	−5.3	−5.3	−2.91
0 −2				−6.61
0 −3				−11.01
0 −4				−16.78
x y		Model 1		
1 0	14.23(1)	14.31(2)	14.27(1)	16.74(1)
2 0	26.25(1)	26.39(2)	26.35(2)	30.25(2)
2 1	30.50(5)	30.60(9)	30.54(6)	34.57(2)
σ_{pH} [e]	0.0047	0.0077	0.0060	0.0150
x y		Model 2		
1 0	14.21(1)	14.29(2)	14.25(2)	16.62(1)
1 −1	8.71(5)	9.0(1)	9.09(7)	12.53(1)
2 0	26.23(1)	26.37(2)	26.33(2)	30.22(1)
σ_{pH} [e]	0.0051	0.0086	0.0078	0.0072

[a] Together with 0.05 mol dm^{-3} KCl to maintain a constant ionic strength of 0.1. [b] Moles of titrant per mole of tdci. [c] $\beta(ML_xH_y) = [M(tdci)_xH_y][M]^{-1}[tdci]^{-x}[H]^{-y}$. [d] Used in both models with fixed formation constants (values from ref. [23], not refined). [e] Definition of σ_{pH} see ref. [22].

Table 6. Potentiometric data (25 °C, μ = 0.1 mol dm^{-3}) and evaluated equilibrium constants for the alkalimetric titrations (0.1 mol dm^{-3} KOH) of **1**, **2**, **3**, and **4a** (estimated standard deviations in parentheses) [43].

metal (compound)	Al (**1**)	Fe (**2**)	Ga (**3**)	In (**4a**)
inert electrolyte	KCl	KCl	KCl	KNO_3
$[M]_t$/mol dm^{-3}	10^{-3}	10^{-3}	10^{-3}	10^{-3}
$[tdci]_t$/mol dm^{-3}	2×10^{-3}	2×10^{-3}	2×10^{-3}	2×10^{-3}
evaluated range [a]	0.0–2.0	0.0–2.0	0.0–2.25	0.0–2.0
no. of data points	75	77	87	77
pK_1 [b]	10.05(2)	10.07(2)	10.03(1)	10.17(2)
pK_2 [b]		11.38(5)		11.29(5)
$\log\beta_2$ [c]	26.30(2)		30.24(1)	28.46(5)
$\log\beta(M(OH)_4)$ [d]	−23.62		−16.78	−21.22
σ_{pH} [e]	0.0089	0.0030	0.0014	0.0028

[a] Moles of titrant per mole of tdci. [b] $pK_i = -\log K_i$, $K_i = [H_{-i}M(tdci)_2][H]-[H_{1-i}M(tdci)_2]^{-1}$. [c] $\beta_2 = [M(tdci)_2][M]^{-1}[tdci]^{-2}$. [d] $\beta(M(OH)_4) = [M(OH)_4]-[H]^4[M]^{-1}$ used as fixed values (from ref. [23], not refined).[e] Definition of σ_{pH} see ref. [22].

Table 7. Potentiometric data (25 °C, 0.1 mol dm^{-3} KCl) and evaluated equilibrium constants of **6**, **7**, and **8** (estimated standard deviations in parentheses).

metal	Ti (**6**)	Sn (**8**)	Ge (**7**)	Ge (**7**)	
titrant	KOH	KOH	KOH	HCl	
[titrant]/mol dm^{-3}	0.1	0.1	0.1	0.1	
$[M]_t$/mol dm^{-3}	5×10^{-4}	5×10^{-4}	5×10^{-4}	5×10^{-4}	
$[tdci]_t$/mol dm^{-3}	10^{-3}	10^{-3}	10^{-3}	10^{-3}	
type of titration	continuous	continuous	continuous	batch	
evaluated range [a]	0.0–2.0	0.0–2.0	0.0–2.0	0.19–2.94	
no. of data points	58	58	58	22	
				Model 1	Model 2
pK_1 [b]	6.67(1)	6.76(1)	6.82(1)		
pK_2 [b]	8.06(1)	8.04(1)	8.10(1)		
pK_3 [b]	9.63(1)	9.69(1)	9.44(1)		
pK_4 [b]	11.17(2)	11.02(2)	10.43(2)		
$\log K_1$ [c]				19.58(4)	19.60(4)
$\log K_2$ [d]					17.44(8)
$\log K_3$ [e]					3.71(5)
σ_{pH} [f]	0.0015	0.0062	0.0071	0.0138	0.0051

[a] Moles of titrant per mole of tdci. [b] $pK_i = -\log K_i$, $K_i = [H_{-i}M(tdci)_2][H][H_{1-i}M(tdci)_2]^{-1}$. [c] $K_1 = [Ge(tdci)_2][H_{-1}Ge(tdci)]^{-1}[tdci]^{-1}-[H]^{-1}$. [d] $K_2 = [Ge(tdci)_2][Ge(tdci)]^{-1}[tdci]^{-1}$. [e] $K_3 = [HGe(tdci)_2][Ge-(tdci)_2]^{-1}[H]^{-1}$. [f] Definition of σ_{pH} see ref. [22].

Calculation of Equilibrium Constants: In this work, all constants are concentration quotients, and pH is defined as $-\log[H]$. pK_w was evaluated from the calibration titrations (Table 8). Consistent models were tested with the computer program SUPERQUAD [20]. Final refinements were performed with the computer program BEST [21] for an optimal σ_{pH} fit [22]. Only the variables as indicated in Tables 5–7 were allowed to vary in the refinement. The constants for the mononuclear hydrolysis products of Ga, Al, and In were taken from ref. [23], and were included as fixed values in the refinement. No significant differences were found by using either BEST or SUPERQUAD for evaluation. The pK_a values of H_3tdci^{3+} were redetermined at 25 °C and various ionic strengths (Table 8) [9,10].

Table 8. pK_a values [a] of H_3tdci^{3+} at 25 °C and various ionic strength μ.

μ/mol dm^{-3}	pK_1	pK_2	pK_3	pK_w	σ_{pH} [d]
0.1 [b]	5.89	7.62	9.68	13.79	0.0023
0.1 [c]	5.86	7.61	9.68	13.79	0.0020
0.2 [b]	6.02	7.72	9.72	13.75	0.0027
0.5 [b]	6.24	7.88	9.81	13.74	0.0024
1.0 [b]	6.46	8.09	9.96	13.78	0.0031

[a] $pK_i = -\log K_i$, $K_i = [H_{3-i}tdci][H][H_{4-i}tdci]^{-1}$, all estimated standard deviations are 0.01 or less. [b] KCl as inert electrolyte. [c] KNO_3 as inert electrolyte. [d] Definition of σ_{pH} see ref. [22].

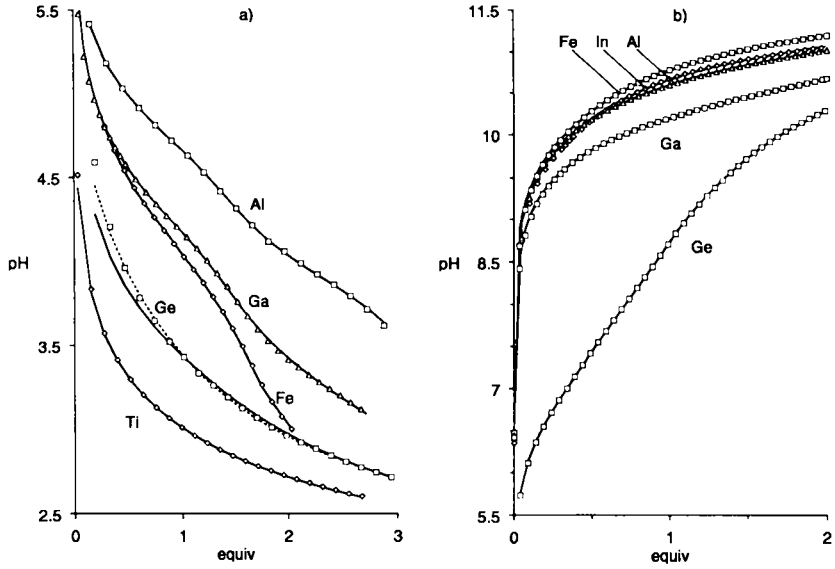

Fig. 1. a) Acidimetric and b) alkalimetric titration curves [43] (25 °C, $\mu = 0.1$ mol dm^{-3}) of the $[M(tdci)_2]^{3+}$ complexes **1**–**3** and **4a** (M = Al^{III}, Fe^{III}, Ga^{III}, In^{III}) and of the $[M(tdci)_2]^{4+}$ complexes **6** and **7** (M = Ge^{IV}, Ti^{IV}); equiv = moles of titrant per mole of tdci. The points represent the experimental values, the solid lines were calculated from the equilibrium constants listed in Tables 5–7. The solid line of the Ti complex represents the simple addition of H^+ to the solvent. The dashed line refers to the extended Model 2 (Table 7) of the Ge complex. Only every second point of the alkaline titrations is shown for clarity. The alkaline titration curves of the Ti and Sn complex are not shown, since they are almost identical to the curve of the Ge complex.

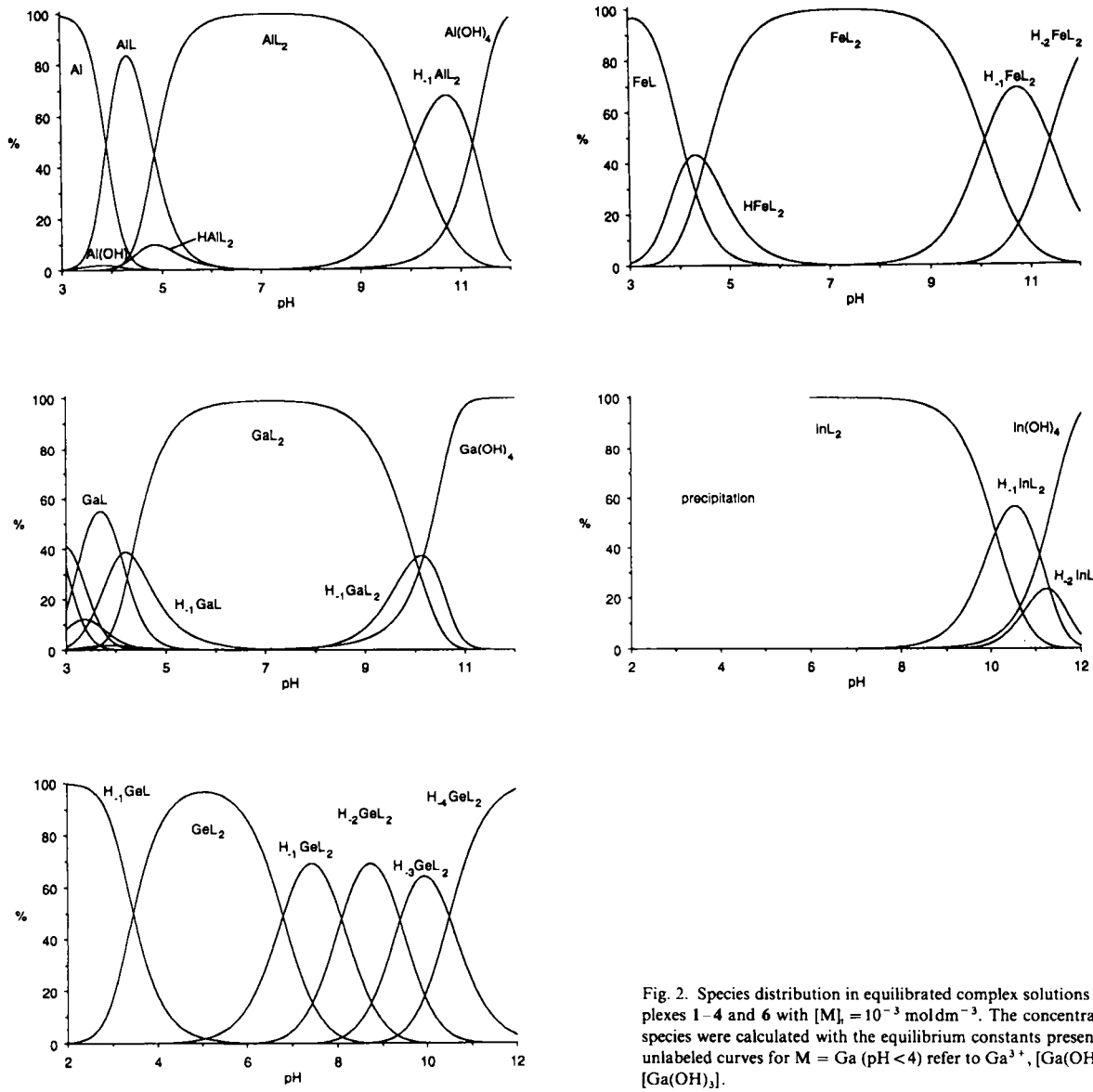

Fig. 2. Species distribution in equilibrated complex solutions of the tdci (= L) complexes **1**–**4** and **6** with $[M]_t = 10^{-3}$ mol dm^{-3}. The concentrations of the individual species were calculated with the equilibrium constants presented in Tables 5–7. The unlabeled curves for M = Ga (pH < 4) refer to Ga^{3+}, $[Ga(OH)]^{2+}$, $[Ga(OH)_2]^+$, and $[Ga(OH)_3]$.

0570-0833/95/0101-0078 $ 10.00+.25/0 Chem. Eur. J. 1995, 1, No. 1

Results

Preparation of Tdci Complexes with Trivalent and Tetravalent Metal Cations: $In(NO_3)_3$, $Tl(NO_3)_3$, the anhydrous chlorides MCl_3 (M = Al, Fe, Ga, In), or MCl_4 (M = Si, Ti, Ge, Sn) and a slight excess of the free ligand were applied as starting materials. The hydrolytic polymerization of the metal cations[24] prior to formation of the target complexes was avoided by the use of dry methanol as solvent. Compounds of the mononuclear bis complexes were prepared by the procedure reported previously for the analogous complexes with taci.[4] However, a significant difference was noted: the taci complexes precipitated immediately after the combination of the two solutions, whereas the tdci complexes remained dissolved. Solid products could be obtained from a mixture of water and EtOH or water and acetone. $[Si(tdci)_2]Cl_4$ (**5**) hydrolyzed in water and was therefore prepared in THF. The Tl complex proved to be unstable and the determination of a defined composition failed. However, the other complexes could conveniently be isolated as crystalline hydrates of the composition $[M(tdci)_2]Cl_3 \cdot 14.5H_2O$ (M = Al (**1**), Fe (**2**), Ga (**3**), In (**4a**)), $[In(tdci)_2]_{1-n}[In(tdci)(H_{-1}tdci)]_n(NO_3)_{3-n} \cdot 13.5H_2O$ ($0 < n \leq 0.4$, **4b**), $[M(tdci)_2]_{1-n}[M(tdci)(H_{-1}tdci)]_nCl_{4-n} \cdot 14.5H_2O$ (M = Ti (**6**), Ge (**7**), $0.2 < n \leq 0.3$), and $[Sn(tdci)_2]Cl_4 \cdot 13.5H_2O$ (**8**). The compounds were characterized by ^1H and ^{13}C NMR spectroscopy (identification of the coordination mode, Table 9), FAB^+ mass spectrometry (evidence for molecular ions $[M(tdci)_2 - xH]^+$, Table 10), and correct elemental analyses.[15] The partial incorporation of deprotonated species in the solid compounds, as observed for **4b**, **6**, and **7**, is well known for taci and tdci complexes. Some of these deprotonated complexes crystallized as well-defined compounds like $[Fe(taci)(H_{-1}taci)](NO_3)_2 \cdot 2H_2O$[25] or $[Cr(taci)(H_{-1}taci)][Cr(taci)_2]_2(SO_4)_4 \cdot 30H_2O$.[1] However, others proved to be mixtures with a variable degree of deprotonation. Particularly for the previously reported $[Ga(taci)_2]_{1-n}[Ga(taci)(H_{-1}taci)]_nX_{3-n}$ (X = Cl, NO_3, $0 < n \leq 0.3$)[4] and **4b**, the composition was poorly reproducible and the degree of deprotonation (n) had to be determined by pH titration for each individual sample.

Table 9. NMR data of tdci, H_3tdci^{3+}, and the complexes $[M(tdci)_2]^{z+}$ (z = 3, 4). Chemical shifts are given relative to [D$_4$](trimethylsilyl)propionate.

compound	^1H NMR H(-C-O)	H(-C-N)	H_3C(-N)	^{13}C NMR cyclohexane ring		H_3C(-N)
tdci	4.58	2.03	2.41	68.8	68.5	44.5
H_3tdci^{3+}	4.94	3.50	3.14	67.0	64.1	44.6
$[Al(tdci)_2]^{3+}$	4.77	2.99	3.03	69.9	66.0	44.0
$[Ga(tdci)_2]^{3+}$	4.87	3.01	3.05	70.3	67.8	44.0
$[In(tdci)_2]^{3+}$	4.92	3.06	3.06	71.3	68.7	44.1
$[Ti(tdci)_2]^{4+}$	5.16	3.60	3.09	68.9	68.4	44.7
$[Ge(tdci)_2]^{4+}$	5.05	3.19	3.08	71.0	68.6	44.9
$[Sn(tdci)_2]^{4+}$	5.15	3.31	3.12	71.4	69.6	44.7

Single crystals of **6**, **7**, and **8** were grown by layering the aqueous complex solution with acetone (4 °C). However, these crystals were very fragile. They dissolved again at room temperature and decomposed immediately after removal from the mother liquor. For the Ti complex, an X-ray structure analysis was performed, which showed unambiguously the presence of mononuclear $[Ti(tdci)_2]^{4+}$ with a Ti–O bond length of 1.94 Å. However, the quality of the structure was not sufficient for publication (R = 12%).

The tdci complexes could readily be dissolved in water. The Si complex **5** decomposed in aqueous solution at pH 7 to form solid SiO_2. The other complex solutions were stable at pH 7 over a period of several weeks and the formation of a solid hydrolysis product was not observed.

Crystal Structure of $[M(tdci)_2]Cl_3 \cdot 15H_2O$ (1–3, 4a; M = Al, Fe, Ga, In): The four compounds were found to be isostructural and isomorphous. The crystals contain mononuclear $[M(tdci)_2]^{3+}$ entities with an approximately octahedral MO_6 coordination sphere. An ORTEP representation is depicted in Figure 3. Six $NH(CH_3)_2^+$ groups were found per complex, and there was no evidence for the presence of any H(-O) position. Clearly, the four metal ions are bound to six fully deprotonated alkoxo groups and a proton transfer from OH to $N(CH_3)_2$ occurred upon coordination. A similar process was previously described for corresponding taci complexes.[4] The metal cations are located on a center of symmetry and on a threefold axis. Thus, the crystallographic symmetry of the complex is S_6 with two independent positions for the two carbon atoms in the dimethylamino group. While the symmetry of the complexes in aqueous solution is fully D_{3d} (confirmed by NMR spectroscopy in D_2O), only pseudo symmetry planes for the single $M(tdci)_2Cl_3 \cdot 15H_2O$ entity could be found in the solid state. Since the packing of crystal structure resulted in the space group $R\bar{3}$, this pseudo symmetry was clearly not crystallographic.

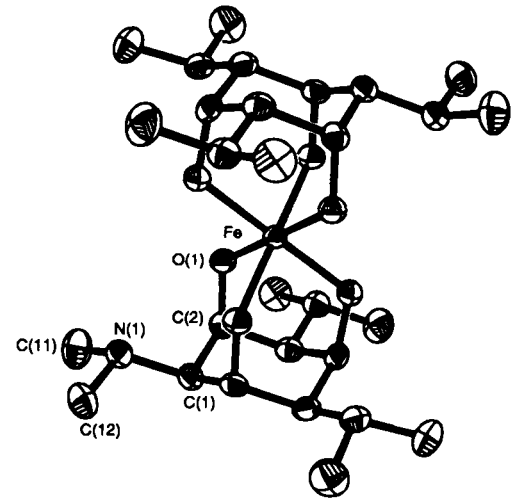

Fig. 3. ORTEP drawing of $[M(tdci)_2]^{3+}$ (M = Al, Fe, Ga, In) with numbering scheme and vibrational ellipsoids at the 50% probability level. Hydrogen atoms are omitted for clarity. The parameters drawn refer to the Fe complex.

In the pseudo-octahedral coordination sphere, the intraligand O-M-O angles are always <90°, whereas the interligand angles O-M-O′ are always >90°.[26] An increasing deviation from 90° is observed with increasing ionic size in the series Al < Ga < Fe < In (see Table 4). For Al, deviation from the octahedral geometry is negligible, whereas for the larger metal cations, significant deviations from regularity is observed. The distortion can be regarded as a stretching along the threefold axis and is a consequence of steric strain in the six-membered chelate rings. The strain increases with increasing ionic size and is generally observed in complexes of taci-type ligands with a type(i) or a type(iv) coordination (Scheme 1) and sufficiently large metal ions.[6] The M–O bond lengths in the tdci complexes ($d(Al^{III})$ = 1.91, $d(Fe^{III})$ = 2.01, $d(Ga^{III})$ = 1.97, and $d(In^{III})$ = 2.14 Å) compare well with the average M–O bond lengths in

corresponding complexes with an octahedral MO_6 coordination ($d_{av}(Al^{III}) = 1.89$,[27] $d_{av}(Fe^{III}) = 2.01$,[28] $d_{av}(Ga^{III}) = 1.97$,[29] and $d_{av}(In^{III}) = 2.14$ Å[30]).

A total of twelve water molecules interact with the $[M(tdci)_2]^{3+}$ entities by hydrogen bonding (Fig. 4). Two types of water molecule can be distinguished, each accounting for six of the

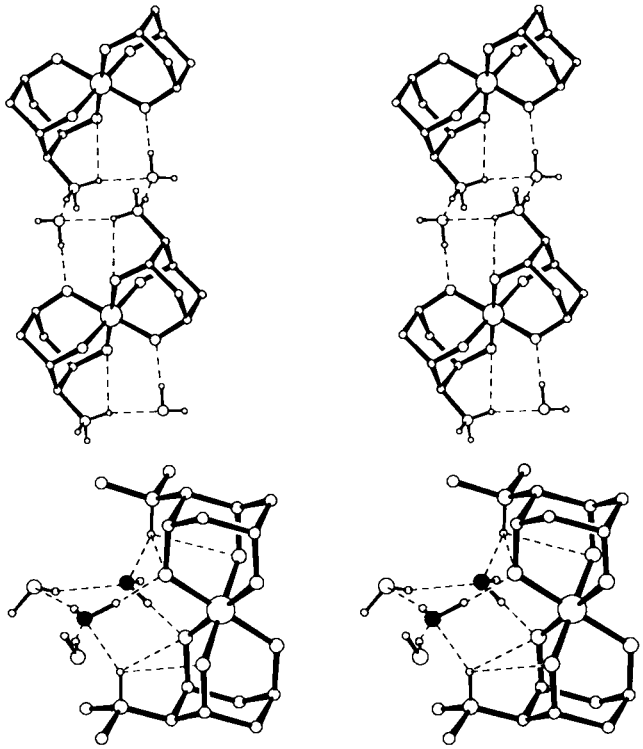

Fig. 4. Hydration of $[Al(taci)_2]^{3+}$ (top) and $[Al(tdci)_2]^{3+}$ (bottom) in the solid state (stereo views). Only a part of the complex molecules is shown for clarity. The oxygen atoms of type 1w are shown as solid spheres those of type 2w as open spheres. Hydrogen bonds are represented by dashed lines.

interacting molecules: a) Type 1w, with an M–O(1w) distance of 3.9 Å, forms a short O(1w)–H···O hydrogen bond to the deprotonated oxygen atom of a ligand molecule and a second O(1w)···H–N hydrogen bond to the protonated dimethylamino group of the other ligand. In addition, two hydrogen bonds are formed to two water molecules of the second 2w type. b) Type 2w water molecules, with an M–O distance of 5.4 Å, show only direct contacts to the 1w water molecules. Hence, the six 1w water molecules can be regarded as a second and the six 2w water molecules as a third coordination sphere around the central metal ion M^{3+}. It is interesting to note that all twelve water molecules and the central M^{III} atom are roughly located in a plane. The deviation from the mean plane defined by the central metal ion and the twelve oxygen positions of the water molecules is ≤ 0.04 Å for O(1w) and ≤ 0.24 Å for O(2w). Hence, the particular structure of the $[M(tdci)_2]^{3+}$ complexes can be described as a sandwich-type structure with a lipophilic shell, formed by the two cyclohexane rings and the twelve peripheral methyl groups, and a hydrophilic pocket formed by the six deprotonated alkoxo groups and the six N–H groups. This hydrophilic pocket is completely filled with the twelve water molecules (Fig. 5). The orientation of the N–H groups and the short N–H···O_{alkoxo} distances of 2.50 and 2.58 Å also indicates the presence of intramolecular hydrogen bonding in the $[M(tdci)_2]^{3+}$ entity. It seems highly probable that a similar type

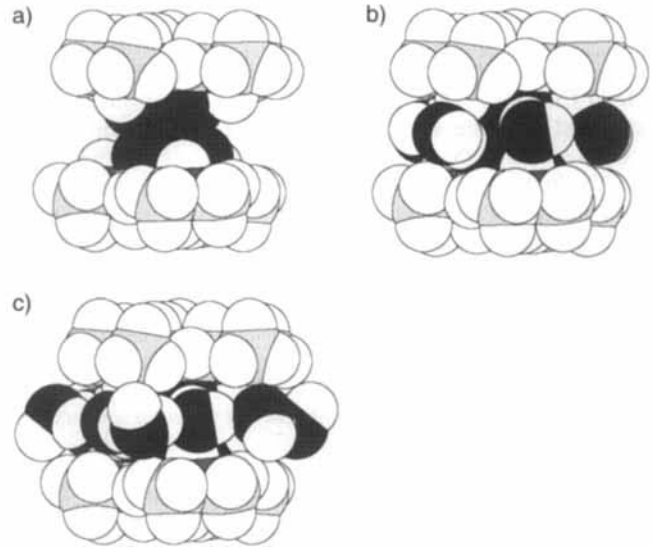

Fig. 5. Hydration of $[M(tdci)_2]^{3+}$ in the solid state (space filling model). Filling of the hydrophilic pocket with water molecules: a) the naked $[M(tdci)_2]^{3+}$ entity; b) $\{[M(tdci)_2]\cdot 6H_2O\}^{3+}$: six water molecules of type 1w form a second coordination sphere; c) $\{[M(tdci)_2]\cdot 12H_2O\}^{3+}$: six additional water molecules of type 2w form a third coordination sphere.

of interaction between water molecules and $[M(tdci)_2]^{3+}$ complexes is also present in solution. We therefore regard the $[M(tdci)_2]\cdot 6H_2O\cdot 6H_2O$ structure as an instructive model for studying solvation effects of such complexes.

Mass Spectrometry: The fast atom bombardment (FAB) ionization technique and the positive ion registration mode was applied to measure the mass spectra of compounds **1**–**8**. A sample of a corresponding $[Tl(tdci)_2](NO_3)_3$ (**9**) complex has been included in this investigation. Table 10 summarizes the major signals together with corresponding assignments. Signals of the pseudo molecular ions $[M(tdci)_2-xH]^+$ where observed with high intensities for all nine compounds. However, close analysis of the isotope patterns revealed the presence of several species with a variable number x of abstracted hydrogen atoms. The problem of ion overlap was solved by means of least-squares calculations (Fig. 6). We explain the predominant formation of $[M^{III}(tdci)_2-2H]^+$ and $[M^{IV}(tdci)_2-3H]^+$ by a partial deprotonation of the peripheral dimethylammonium groups, as required for the generation of a monopositive species. The observation of increased amounts of $[Tl(tdci)_2]^+$ and $[Ti(tdci)_2-2H]^+$ can be interpreted as a reduction of the metal cation by the glycerol matrix, resulting in the formation of Tl^I and Ti^{III}. The addition of a neutral hydrogen atom is therefore a combination of an electron uptake by the metal and a proton uptake by the partially deprotonated ligand. The reverse reaction, that is, the abstraction of H_2 from $[M^{III}(tdci)_2-2H]^+$ or $[M^{IV}(tdci)_2-3H]^+$ is also observed. We explain this elimination by an additional deprotonation of a dimethylammonium group, followed by a hydride abstraction from one of the methyl groups. Hydride abstraction is frequently observed in the FAB mass spectra of carbohydrates and related compounds.[31] There is, of course, no experimental evidence to exclude an alternative mechanism consisting of a twofold deprotonation of the ligand and a release of two electrons from the metal center. However, the formation of oxidized cations like Si^{VI}, Ge^{VI} or Al^V, Ga^V, etc., is highly improbable. The postulated dehydrogenation of the C–N single bond is further supported by the observed elimination of CH_2 ($\Delta m/z = -14$), which can be un-

0570-0833/95/0101-0080 $ 10.00+.25/0 Chem. Eur. J. 1995, 1, No. 1

Table 10. FAB$^+$ Data for the bis complexes $[M(tdci)_2]^{z+}$ (M = Al, Fe, Ga, In, Tl, Si, Ti, Ge, Sn; z = 3, 4).
a) Analysis of the signals of the pseudo molecular ions, taking into consideration a superposition of several species ($[M(tdci)_2-xH]^+$, $0 \le x \le 5$). The relative abundance of each species was established by least squares calculations $\sum_i (I_{obs}-I_{calcd})^2$ = min.

species	Al	Fe	Ga	In	Tl	Si	Ti	Ge	Sn
$[M(tdci)_2]^+$	–	–	–	–	100	–	–	–	–
$[M(tdci)_2-H]^+$	–	50	–	–	–	–	–	–	–
$[M(tdci)_2-2H]^+$	100	100	100	100	14	–	28	–	–
$[M(tdci)_2-3H]^+$	–	15	–	–	–	100	100	100	100
$[M(tdci)_2-4H]^+$	6	9	7	10	3	–	–	–	–
$[M(tdci)_2-5H]^+$	–	–	–	–	–	16	9	18	10
R/% [a]	1.9	4.3	2.3	7.5	8.3	4.6	2.1	3.5	1.8
m/z, range	545–549	573–578	587–593	633–637	721–730	543–550	563–571	587–596	633–644

[a] $R = \sum|I_o-I_c|/\sum|I_o|$, see ref. [13].

b) Relative Intensities of the major ion associates, glycerol (= glyc) adducts, and fragmentation products. Ions, which differ only in the amount of hydrogen are treated as one single component. The intensity of the most abundant isotopomer of such a signal is compared with the most abundant isotopomer of the pseudo-molecular ion $[M(tdci)_2-xH]^+$ (=100%). The data of the Fe complex are reported in ref. [9].

assignments	Al	Ga	In	Tl	Si	Ti	Ge	Sn
$[M(tdci)_2Cl_2-(x-2)H]^+$	–	5	19	–	–	–	–	–
$[M(tdci)_2Cl-(x-1)H]^+$	9	12	16	–	22	–	6	8
$[M(tdci)_2-xH]^+$	100	100	100	100	100	100	100	100
$[M(tdci)_2-xH-14]^+$	13	14	14	11	6	18	16	16
$[M(tdci)_2Cl-(x-1)H-99]^+$	10	9	12	–	–	16	11	12
$[M(tdci)(glyc)(H_2O)_2-xH]^+$	8	–	7	–	–	10	7	–
$[M(tdci)(glyc)-xH]^+$	7		8	42	8	6		5
$[M(tdci)(H_2O)-xH]^+$	19	22	8	–	16	–	21	2
$[M(tdci)-(x-2)H]^+$	–	–	47	131	–	–	28	97

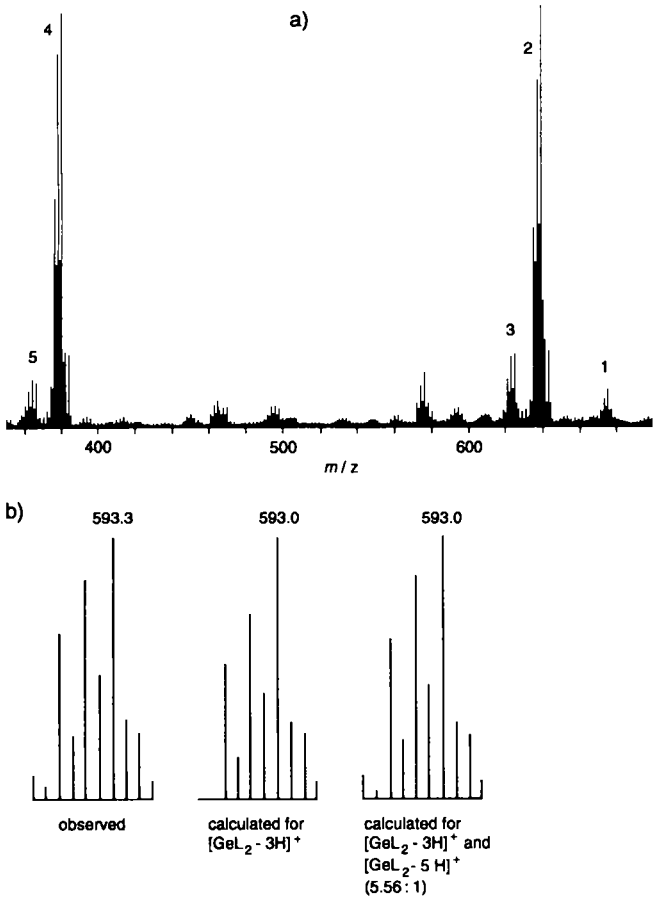

Fig. 6. FAB$^+$ MS of $[Sn(tdci)_2]Cl_4 \cdot 14H_2O$ and $[Ge(tdci)_2]Cl_4 \cdot 14H_2O$. a) Spectrum of the Sn complex. Assignments: 1, $[Sn(tdci)_2Cl-2H]^+$; 2, $[Sn(tdci)_2-xH]^+$ (x = 3, 5); 3, $[2-CH_2]^+$; 4, $[Sn(tdci)-yH]^+$ (y = 1, 3); and 5 $[4-CH_2]^+$. b) Comparison of the observed signal of the pseudo molecular ion $[Ge(tdci)_2-xH]^+$ with the calculated isotope distribution for $[Ge(tdci)_2-3H]^+$ (R = 12.7%) and a 5.56:1 mixture of $[Ge(tdci)_2-3H]^+$ and $[Ge(tdci)_2-5H]^+$ (R = 3.5%).

derstood as a solvolysis reaction of the $H_2C=N(CH_3)$- fragment.

Dissociation of one tdci molecule resulted either in the formation of $[M(tdci)(H_2O)-xH]^+$ (M = Al, Ga, x = 2; M = Si, x = 3) or $[M(tdci)-(x-2)H]^+$ (M = Tl, x = 2; M = Sn, x = 3). For In and Ge, both types of ligand dissociation have been observed. In the first type of fragmentation, a d^{10} cation is formed, which we tentatively formulate as a tetrahedrally coordinated hydroxo complex $[M(H_{x-1}tdci)(OH)]^+$. In the second type of fragmentation, the metal center is reduced to a $d^{10}s^2$ cation. The increased tendency in the order Al,Ga $\ll$ In < Tl and Si $\ll$ Ge < Sn to form mono or divalent cations with a $d^{10}s^2$ electron configuration, as observed in the mass spectra, is a well established characteristic of the Group 13 and Group 14 elements. The reduction of the In, Ge, and Sn complexes was strictly coupled with an elimination of one tdci ligand; this indicates the formation of species with a trigonal-pyramidal geometry and a stereochemically active lone pair. A reduction of the bis complexes was not observed. In contrast, reduced bis complexes were formed in the case of Ti and Tl. Moreover, the reduction of the Ti^{IV} complex resulted only in the formation of Ti^{III}, whereas Ge^{IV} and Sn^{IV} formed exclusively divalent species.

Scheme 3 summarizes the fragmentation processes observed in the FAB spectra of **1**–**9** (Table 10). Five different types of reactions can be distinguished:

a) The simple deprotonation of the peripheral dimethylammonium groups. This ubiquitous reaction is necessary for charge adjustment. Three peripheral dimethylammonium groups per ligand serve as a reservoir of ionizable protons. Thus, monopositive ions can be generated regardless of the charge of the metal center.

b) Addition of HCl (Cl^- and H^+) to the bis complexes. It is of course not possible to decide wether Cl^- is directly bound to the metal ion or wether it forms a hydrogen bond to the ligand. A coordination number of 7 seems very unlikely for Al^{III}, but more probable for In^{III}.

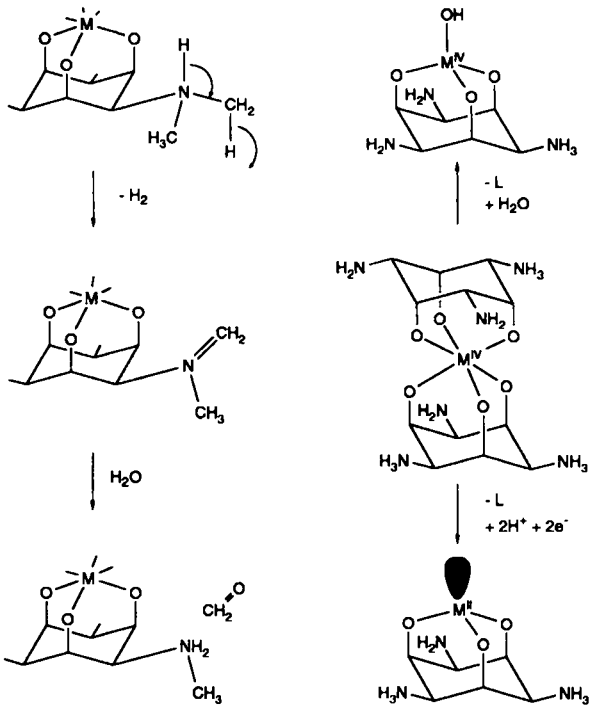

Scheme 3. Fragmentation processes observed in the FAB spectra of **1**–**9**.

c) Reduction of the metal cation. It is well known that the glycerol matrix can act as a strong reducing agent under FAB conditions. This reactivity is attributed to the formation of organic radicals, generated during the bombardment of the sample.

d) Elimination of one ligand molecule. For all metal ions except Ti^{IV}, the formation of 1:1 complexes has been observed in the FAB spectra. The eliminated ligand can be replaced by a solvent molecule like H_2O or glycerol (or both). However, for In^{III}, Tl^{III}, Ge^{IV}, and Sn^{IV}, a reductive elimination (combination of c) and d)) can also occur. In this case the eliminated ligand is not substituted due to a stereochemically active lone pair.

e) Fragmentation reactions within the ligand. These processes probably all start with a hydride abstraction from a methyl group. The elimination of CH_2 or even the rupture of the cyclohexane ring then follows. Evidence for the latter step comes from $[M(tdci)_2Cl-99]^+$, which might be formed by the elimination of $O{=}CH{-}CN(CH_3)_2{=}CH_2$.

All these reactions are typical for solution chemistry. Thus, our results clearly suggests that the various species observed in the spectra are generated in the matrix rather than in the gaseous phase. The particularly low abundance of mononuclear Tl^{III}–tdci complexes is thus a strong indication of the low stability of $[Tl(tdci)_2]^{3+}$ in solution.

Reactions in Aqueous Solution and Determination of Equilibrium Constants: $[Si(tdci)_2]Cl_4$ and $[Tl(tdci)_2](NO_3)_3$ decomposed rapidly in water, and the formation constant of these complexes could not be determined. However, compounds **1**–**4** and **6**–**8** proved to be of sufficient stability to allow a variety of reactions in aqueous solution to be investigated. These complexes could readily be dissolved in D_2O, and NMR spectroscopic measurements of the resulting clear and almost neutral solutions established the presence of the intact bis complexes at pH 7 (Table 9). Signals corresponding to the free ligand, which would be expected to appear upon decay, were not observed at all.

A variety of acidimetric titrations (25 °C, $\mu = 0.1$ M) were performed to investigate the reactivity below pH 7 (Tables 5 and 7, Fig. 1).[43] However, an evaluation of the titration curves of the In^{III} complexes **4a** and **4b** was not possible, because solid hydrolysis products precipitated immediately after the addition of acid to the complex solution. The solutions of the Ga complex **3** also hydrolyzed slowly below pH 5. A colorless solid precipitated after a period of several days and was identified as $Ga(OH)_3$.[32] However, the hydrolytic decomposition of **3** was sufficiently slow to allow the detection of a rapid preequilibrium exclusively involving mononuclear species. The reliability of these measurements was confirmed by performing two different titrations with equilibration times of 15 and 60 min per point, respectively. Although the results of the slower titration were somewhat less consistent, indicating that some hydrolytic decomposition had already taken place, the evaluated formation constants of the two experiments did not differ significantly. A buffer region was observed at pH 4, which was interpreted in terms of ligand dissociation resulting in the formation of a 1:1 complex. Two different models were tested in the final refinement. In both models, the mononuclear hydrolysis products $[Ga(OH)]^{2+}$, $[Ga(OH)_2]^+$, $[Ga(OH)_3]$, and $[Ga(OH)_4]^-$ (included with fixed values) as well as $[Ga(tdci)_2]^{3+}$ and $[Ga(tdci)]^{3+}$ were taken into consideration. In addition, Model 1 included a protonated species $[HGa(tdci)_2]^{4+}$, whereas the deprotonated species $[H_{-1}Ga(tdci)]^{2+}$ was used for Model 2. The latter was favored owing to a systematically lower σ_{pH}.[22]

There was no indication for hydrolytic polymerization of the dissolved compounds **1**, **2**, **6**, **7**, and **8** at any pH in the range $2 < pH < 12$. The acidimetric titrations of the Al^{III} complex **1**, the Fe^{III} complex **2**, and the Ge^{IV} complex **7** were performed in batches. At least 72 h was allowed for complete equilibration. The observation of a buffer region was again interpreted in terms of a ligand dissociation. The evaluation of the results for **1** and **2** has already been reported.[9] In this previous investigation, it was, however, not possible to assign unambiguously the composition of a minor species observed in the titration of **1**. We therefore repeated these measurements using three different concentrations and established that a small amount of the protonated bis complex $[HAl(tdci)_2]^{4+}$, rather than $[H_{-1}Al(tdci)]^{2+}$, is formed in slightly acidic solution. The acidimetric titrations of the Sn and Ti complexes **6** and **8** corresponded to a simple addition of the titrant to the solvent; thus, no decay of these complexes occurred even at pH 3. However, for the Ge^{IV} complex **7** the drop in pH was much less significant; this indicates that H^+ was consumed during the acidimetric titration. In accordance with the observed reactivity in the FABMS (Table 10b), this result was interpreted as a ligand dissociation reaction to form $[H_{-1}Ge(tdci)]^{3+}$ as additional species (Model 1), which we tentatively regard as a tetrahedrally coordinated $[Ge(tdci)(OH)]^{3+}$. However, a rather poor fit was obtained for this model with particularly large deviation of pH_{calc} from pH_{obs} at the beginning of the titration (Fig. 1a). The consideration of polynuclear species did not help reduce this deviation; however, the curve could satisfactorily be explained if the additional presence of the protonated bis complex $[HGe(tdci)_2]^{5+}$ and the 1:1 complex $[Ge(tdci)]^{4+}$ is postulated (Model 2). Although Model 2 resulted in an acceptable fit, it is dubious for chemical reasons: The different behavior of the Ge complex on the one hand and the Ti and Sn complexes on the other is understandable in terms of the increased tendency of Ge^{IV} to form tetrahedral species, thus promoting the formation of a 1:1 complex. However, it is not clear at all why Ge^{IV} should form a protonated bis complex $[HGe(tdci)_2]^{5+}$, whereas Ti^{IV} and Sn^{IV} do not. On the other hand, it is noteworthy that iden-

0570-0833/95/0101-0082 $ 10.00+.25/0 Chem. Eur. J. 1995, 1, No. 1

tical values, within statistical levels of significance, are obtained for $\beta([H_{-1}Ge(tdci)]^{3+})$ by using either Model 1 or Model 2 for evaluation (Table 7). The formation of $[H_{-1}Ge(tdci)]^{3+}$ in slightly acidic solution, as well as the value for its formation constant, should therefore be regarded as having been conclusively established. It should also be noted that the partial dissociation of tdci in acidic solutions was confirmed by NMR spectroscopy (see below).

Alkalimetric titrations of $[Fe(tdci)_2]^{3+}$ revealed the deprotonation of two peripheral $-NH(CH_3)_2^+$ groups (Table 6, Fig. 1b). There was no evidence for any ligand dissociation. The complex $[Al(tdci)_2]^{3+}$ was, however, completely converted to $[Al(OH)_4]^-$ at high pH [Eq. (a)]. Since the formation constant of the tetrahydroxo complex is known, the competition between OH^- and tdci as ligands allowed the determination of $\log\beta_2(Al(tdci)_2) = 26.3$.[33] This result is in good agreement with the average value of 26.33, as obtained from the acidimetric titrations. In addition, the deprotonation of one $-NH(CH_3)_2^+$ group ($pK_1 = 10.05$) was observed. In the case of the Ga^{III}, a related, even more stable complex, $[Ga(OH)_4]^-$, was formed [Eq. (b)]. The formation constant of $[Ga(tdci)_2]^{3+}$ was checked by alkalimetric titrations in the same way as for $[Al(tdci)_2]^{3+}$.[33, 34] The value $\log\beta_2(Ga(tdci)_2)$ (30.24) is in excellent agreement with the result obtained from the acidimetric titration over 15 h ($\log\beta_2 = 30.25$). Again, a deprotonation of one $-NH(CH_3)_2^+$ group could be observed. The evaluated pK_1 value (10.03) compares well with the corresponding values of the Fe and the Al complexes. The formation constant of $[In(OH)_4]^-$ has not been established with the same accuracy as the corresponding values for Al^{III} and Ga^{III}.[24] Therefore, the titration shown in Equation (c) allowed only an approximate estimation of $\beta_2(In(tdci)_2)$. Deprotonation of $[In(tdci)_2]^{3+}$ was also observed, and the evaluated pK_1 (10.12) was again in good agreement with the corresponding values for Fe^{III}, Al^{III}, and Ga^{III}. The alkalimetric titrations of $[Ti(tdci)_2]^{4+}$, $[Ge(tdci)_2]^{4+}$, and $[Sn(tdci)_2]^{4+}$ resulted in the determination of four pK_a values; this indicates that a subsequent deprotonation took place. In strongly alkaline solution the neutral $[H_{-4}M(tdci)_2]$ ($= [M(H_{-2}tdci)_2]$) was formed. As expected, the evaluated pK_a values do not differ significantly for the three complexes. They are, however, considerably lower than the values observed for the complexes with the trivalent cations. The alkalimetric titrations of **6**–**8** gave no indication for any ligand dissociation above pH 7.

$$[Al(tdci)_2]^{3+} + 4OH^- \longrightarrow [Al(OH)_4]^- + 2tdci \quad (a)$$

$$[Ga(tdci)_2]^{3+} + 4OH^- \longrightarrow [Ga(OH)_4]^- + 2tdci \quad (b)$$

$$[In(tdci)_2]^{3+} + 4OH^- \longrightarrow [In(OH)_4]^- + 2tdci \quad (c)$$

NMR Studies: To verify qualitatively the results of the potentiometric studies, a series of ^1H NMR spectra of **1**, **3**, **4a**, and **7** were measured in D_2O and variable pD.

The decomposition of the Ge complex **7** in the acidic range was investigated by the successive addition of DCl to the complex solution. At pD 7, the three signals of the bis complex were observed exclusively. Upon addition of DCl, additional signals of free H_3tdci^{3+} appeared, whereas the amount of Ge-bound tdci decreased continuously. It was, however, not possible to observe individual signals for different Ge–tdci complexes. At pD 1.3, the signals of the complex were no longer visible ($\leq 5\%$); this indicated that complete decomposition had taken place.

The spectra of the Al complex are shown in Figure 7. In the range $7 < pD < 10$, the complex exhibited three signals at $\delta = 4.77$, 3.03, and 2.99, which were assigned to H(-C–O), CH_3(-N), and H(-C–N) respectively. At higher pD, the signals of the complex shifted towards lower field. This effect was particularly pronounced for H(-C–N) and CH_3(-N). The signal of the H(-C-O) hydrogens was much less affected. The sigmoid shape of the curves δ vs pD, together with the observed midpoint at about pD 11 is indicative of a deprotonation of the dimethylammonium groups in the range $10 < pD < 12$. Above pD 11, the signals of the complex decreased steadily with increasing pD, and an increasing amount of the free ligand was observed. The liberation of free tdci is obviously coupled with the formation of $[Al(OH)_4]^-$. This could nicely be confirmed by ^{27}Al NMR spectroscopy (Fig. 8). As is well known, different coordination numbers of Al^{III} can easily be distinguished by different ^{27}Al chemical shifts: octahedrally coordinated Al^{III} is observed at about $\delta = 0$, whereas tetrahedrally coordinated Al^{III} appears at $\delta = 80$. Moreover, the line width of the signals is indicative of the symmetry of the coordination sphere: complexes with low symmetry have broad signals due to quadrupolar relaxation effects of the ^{27}Al nucleus; high symmetry of the coordination sphere results in a low electric field gradient at the

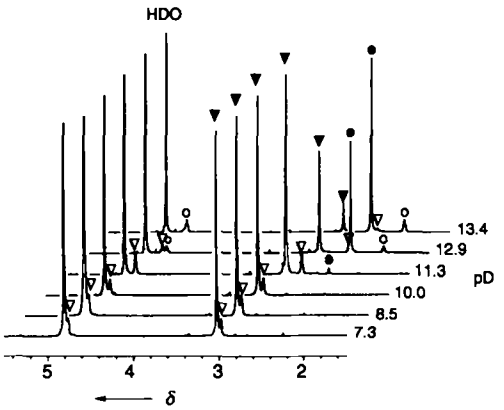

Fig. 7. ^1H NMR spectra (D_2O, 25 °C) of $[Al(tdci)_2]Cl_3 \cdot 15H_2O$ at different pD. $[Al]_t = 0.03$ mol dm^{-3}. Circles refer to the free ligand, triangles to the complex. The solid figures refer to the dimethylamino groups, the open figures to the ring protons.

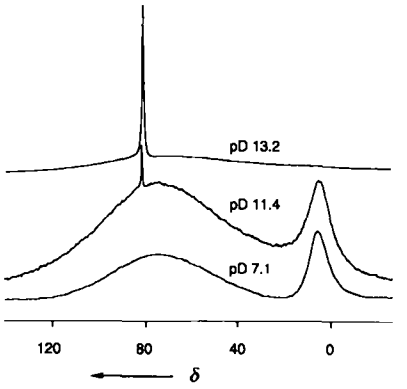

Fig. 8. ^{27}Al NMR spectra (D_2O, 25 °C) of $[Al(tdci)_2]Cl_3 \cdot 15H_2O$ at different pD. $[Al]_t = 0.1$ mol dm^{-3}. The broad signal at $\delta \approx 75$ originates from an extraneous source of Al,[35] and was also present in the spectrum of a blank D_2O solution.

nucleus and thus in a low relaxation rate and sharp signals. For $[Al(tdci)_2]^{3+}$, only one signal at $\delta = 4$ with a moderately small line width ($W_{1/2} = 700$ Hz) could be observed at pD 7. This is consistent with the postulated D_{3d} symmetry of this complex. The sample with pD = 11.4 showed the same signal as for the octahedral $[Al(tdci)_2]^{3+}$ at $\delta = 4$ ($W_{1/2} = 650$) together with a sharp signal at $\delta = 80$ ($W_{1/2} = 40$ Hz), which is typical for $[Al(OH)_4]^-$. Finally, at pD = 13.2 only the sharp signal of $[Al(OH)_4]^-$ was observed. Hence, the ^1H and ^{27}Al NMR data are in excellent agreement with the proposed model, obtained from the titration experiment, in which a peripheral dimethylammonium group is deprotonated and $[Al(tdci)_2]^{3+}$ is converted to $[Al(OH)_4]^-$. An analogous ^1H NMR spectroscopic study was performed for $[Ga(tdci)_2]^{3+}$ and $[In(tdci)_2]^{3+}$. The spectra may be obtained as supplementary material. The Ga complex behaved exactly in the same way as reported here for Al. The main reactions in the case of $[In(tdci)_2]^{3+}$ were also deprotonation of the dimethylammonium groups (pD > 10) and liberation of free tdci (pD > 10.5). However, in strongly alkaline solutions (pD > 12.5) the signal of an additional minor species was observed. It should be noted that such a species was not considered in the alkalimetric titration experiments. This fact does not, however, necessarily contradict the NMR result, since the titrations were performed at much lower concentrations and in a different medium (0.1 mol dm^{-3} KNO_3 vs. D_2O without inert electrolyte). The absence of this additional species in the more dilute solution would be particularly reasonable if it were an oligonuclear complex, since dilution generally diminishes formation of polynuclear species.

Molecular Mechanics Calculations: The strain energy $\sum U$ was calculated as a function of the metal ionic radius for the following types of bis complexes (Fig. 9): a) taci and tdci complexes with a bis-type(iv) coordination with deprotonated oxygen donors, b) taci complexes with a type(i)–type(iv) coordination where the three coordinated oxygens are again deprotonated, and c) taci complexes with a bis-type(i) coordination. The strain energy $\sum U$ includes deformation of bond angles and bond lengths, torsional strain within the ligands, and van der Waals repulsions between the donor atoms in the coordination sphere and, more importantly, between hydrogen atoms attached to these donor atoms. Other types of interactions are not considered. It must be emphasized that the calculations were performed for a generalized metal ion. Variation of the force constants of metal–ligand bonds and angles resulted in considerable changes of the absolute values presented in Figure 9. However, the positions of the minima as well as the relative energy levels of the three categories of complexes are remarkably insensitive to such alterations.

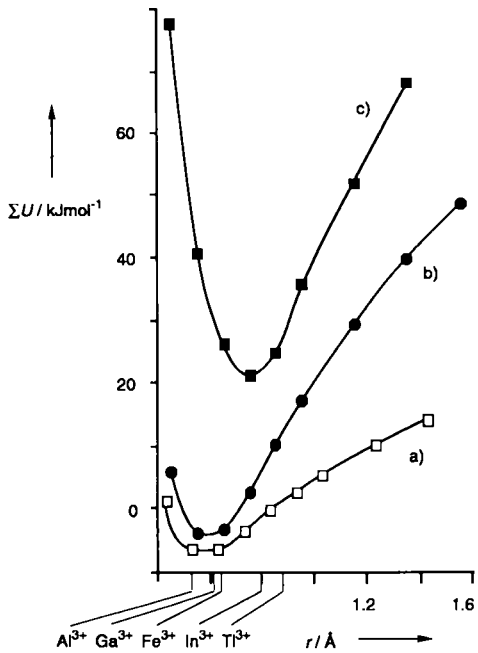

Fig. 9. Molecular mechanics calculations for complexes $[M(taci)_2]^{z+}$ with a) a bis-type(iv), b) type(i)–type(iv), and c) a bis-type(i) structure. The ligands with a type(iv) structure coordinate in the zwitterionic form with deprotonated oxygens and protonated nitrogens. The strain energy $\sum U$ is shown as a function of the ionic radius r [36].

The most important contribution to the strain energy of a bis complex originates from van der Waals interactions, which are slightly attractive when the distances between the atoms are larger than the sum of the van der Waals radii, but become considerably repulsive for shorter distances. This effect is particularly pronounced for complexes of category c) (N_6 coordination) where the strain energy increases steeply when the ionic radius decreases below 0.7 Å owing to increased repulsions between N–H groups. Additional strain is attributed to the exclusive formation of six-membered chelate rings in the complexes of the three categories a)–c), resulting in an adamantane-like structure. Adamantane itself ($M = C^{4+}$, $r_C = 0.15$ Å) is free of strain. However, with increasing ionic radius, the geometry of the chelate rings are subjected to distortion, and increased steric strain is observed for large metal cations. Again, this effect is more pronounced for complexes with coordinated nitrogen donors. Hence, if one considers only the geometric properties of taci and tdci, the results presented in Figure 9 show clearly that very small metal ions bind preferably either to six deprotonated oxygens (bis-type(iv)) or to three nitrogens and three deprotonated oxygens (type(i)–type(iv)).

Discussion

Site Selection: The remarkable metal-binding properties of taci are based on the four different binding sites (i)–(iv) (Scheme 1). In the present investigation, particular attention was given to the sites (i) and (iv), since for steric reasons small metal ions with an ionic radius of 0.8 Å or less, which have been used in this study, preferably bind to three axial donor groups.[18] The molecular mechanics calculations clearly show that in a bis complex of a small cation like Al^{3+}, the bis-type(i) coordination is disfavored owing to considerable repulsion between N–H hydrogen atoms. A type(i)–type(iv) or a bis-type(iv) coordination is much more favorable, particularly when the oxygen donors are deprotonated, which is always the case for trivalent cations. For larger metal ions, this type of repulsion is reduced and a bis-type(i) coordination would be possible. The observed coordination modes in the bis taci complexes of Al^{III}, Ga^{III}, Fe^{III}, In^{III}, and Tl^{III} agree well with this result (Table 11). The very small Al^{III} has a bis-type(iv) coordination, cations of intermediate size, Ga^{III} and Fe^{III}, have a type(i)–type(iv) coordination, and the larger In^{III} and Tl^{III} have bis-type(i) coordination. Thus, going from taci to tdci, the blocking of site (i) generates a ligand with a particularly high selectivity for very small metal ions.

The selection of the coordination site (reaction 1, Scheme 4) is, however, not only based on steric requirements, it is also governed by the different affinities of the metal cations towards nitrogen and oxygen donors. This affinity can be expressed in terms of the equilibrium constant $K(2)$ of reaction 2 (Scheme 4),

0570-0833/95/0101-0084 $ 10.00+.25/0 Chem. Eur. J. 1995, 1, No. 1

Table 11. Correlation of the observed structure types in taci and tdci complexes with the individual affinity of a metal cation for neutral sp^3 nitrogen donors or negative oxygen donors as expressed by the equilibrium constant $K(2)$ of the reaction $[M-NH_3]^{z+} + H_2O \rightleftharpoons [M-OH]^{z-1} + NH_4^+$ for various metal cations.

M	log $K(2)$	taci	tdci	ref.
Mn^{2+}	−2.3	bis-type(i)		[37]
Fe^{2+}	−1.6	bis-type(i)		[37]
Co^{2+}	−2.4	bis-type(i)		[37]
Ni^{2+}	−3.4	bis-type(i)		[2]
Cu^{2+}	−2.4	bis-type(i)		[2]
Zn^{2+}	−2.0	bis-type(i)		[2]
Cd^{2+}	−3.1	bis-type(i)		[6]
Al^{3+}	3.5	bis-type(iv)	bis-type(iv)	taci: [4], tdci: this work
Cr^{3+}	1.8	bis-type(iv) and typ(i)-type(iv)		[1]
Fe^{3+}	3.2	type(i)-type(iv)	bis-type(iv)	taci: [25], tdci: this work
Co^{3+}	0.3	bis-type(i)		[3]
Ga^{3+}	2.4	type(i)-type(iv)	bis-type(iv)	taci: [4], tdci: this work
In^{3+}	1.2	bis-type(i)	bis-type(iv)	taci: [40], tdci: this work
Tl^{3+}	−0.3	bis-type(i)	-	[4]

where the monodentate OH^- and NH_3 stand for a deprotonated hydroxyl group and amino group, respectively. The equilibrium constant $K(2)$ may thus be regarded as a measure of the affinity for the individual affinity of a metal ion for the two types of donor atoms in taci type ligands. Values for $K(2)$, which

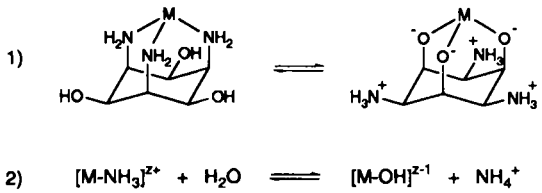

Scheme 4.

can readily be calculated from the formation constants of hydroxo and amine complexes,[38] are collected in Table 11. These data show a rather high affinity of the large and relatively soft In^{III} and Tl^{III} for nitrogen donors and a high preference of the small and hard Al^{III} for oxygen donors. Thus, for cations like Al^{3+} or Ti^{4+} the low-strain geometry of the bis-type(iv) coordination is paralleled by the favorable binding of such ions to deprotonated oxygen donors. The combination of these two requirements is thus responsible for the pronounced selectivity of tdci for highly charged, hard and small metal cations.

Design of Specific Chelators: MM calculations were performed to investigate the difference in energy of the two chair conformations **a** and **b** (Scheme 2) for a variety of taci-type ligands as a function of different substituents. As was shown previously,[6] the two conformers of taci with either OH or NH_2 groups in axial positions have almost the same energy. Both conformers are significantly stabilized by intramolecular hydrogen bonds. The results presented in this paper (Table 12) reveal, however, that both forms can be destabilized considerably by sufficiently bulky substituents. This is important for the specific modification of the metal-binding properties (Scheme 2). The alkylation of the three hydroxyl groups, for instance, disfavors the conformer with three axial oxygens. Moreover, in such ligands, the generation of a negative charge on the oxygens is no longer possible. Thus, such a ligand should bind preferably to metal ions with a high affinity for nitrogen donors. On the other hand,

Table 12. Selective stabilization of one of the two chair conformations of taci and some methylated derivatives. The differences of strain energy $\Delta(\sum U)$ of the two conformations as obtained by molecular mechanics calculations were used to estimate $\Delta G \approx \Delta H \approx \Delta(\sum U)$. The values of $\Delta(\sum U)$ refer to the reaction **a** $\rightleftharpoons$ **b** as shown in Scheme 2; i.e., positive values indicate a stabilization of the conformer with the three nitrogens in equatorial position.

substituents		$\Delta\sum U$/kJ mol^{-1}
-OH	$-NH_2$	+1.9
-OH	$-N(CH_3)_2$	+69.3
$-OCH_3$	$-NH_2$	−34.4
$-CH_3$	$-NH_2$	−37.0

in ligands with alkylated amino groups, like tdci, the conformer with three axial nitrogens is disfavored. Consequently, such ligands will selectively bind oxophilic metal ions. The introduction of such substituents can easily be achieved by the well-known standard procedures of synthetic organic chemistry. Since taci is now readily available,[3] these considerations open attractive routes for the design of new ligands with distinctive metal-binding properties.

The *trans* Influence of Coordinated Alkoxo Groups: A survey of metal–ligand bond lengths in $[M(taci)_2]^{3+}$ and $[M(tdci)_2]^{3+}$ complexes, including some results from previous contributions of this series, is presented in Figure 10. The M–O bond lengths

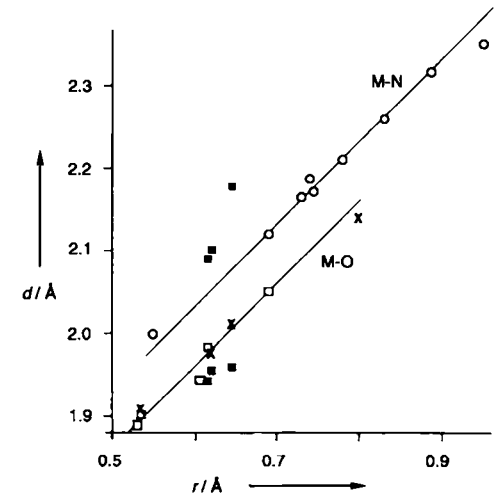

Fig. 10. M–O and M–N bond lengths in the complexes $[M(taci)_2]^{z+}$ and $[M(tdci)_2]^{z+}$ as a function of the ionic radius.[36] The coordinated oxygens in this compilation are all deprotonated (zwitterionic form). Open circles: taci complexes with a bis-type(i) structure (from left to right): Co^{III}, Ni^{II}, Cu^{II}, Zn^{II}, Co^{II}, Fe^{II}, Mn^{II}, Tl^{III}, Cd^{II} [2,3,4,6,37]. Solid squares: taci complexes with a type(i)–type(iv) structure (M–N bonds top, M–O bonds bottom, from left to right): Cr^{III}, Ga^{III}, Fe^{III} [1,4,25]. Open squares: taci complexes with a bis-type(iv) structure (from left to right): Ge^{IV}, Al^{III}, Ti^{IV}, Cr^{III}, Sn^{IV} [1,4,37]. X: tdci complexes with a bis-type(iv) structure (from left to right): Al^{III}, Ga^{III}, Fe^{III}, In^{III}.

d(M–O) of bis-type(iv) complexes (MO_6 coordination with deprotonated oxygens) is linearly dependent on the ionic radius r_M [Eq. (1)].[36] The observed unit slope indicates a constant

$$d(M-O) = 1.36\ \text{Å} + r_M \quad (1)$$

contribution of the oxygen donors to the total length of the M–O bond. Differences between taci and tdci complexes are not significant. An analogous relation is also observed for bis-

type (i) complexes [Eq. (2)]. For taci complexes with a type (i)–type (iv) structure (N_3O_3 coordination with deprotonated oxygens), however, we note significant deviations from Equations (1) and (2) for the M–O as well as the M–N bond lengths. The former are generally slightly shorter than the calculated values obtained from Equation (1). Additional experimental support for a shortening of the M–O bonds in a *fac* MN_3O_3 moiety is provided by the observation of generally longer M–O bond lengths in the corresponding tdci complexes with an MO_6 coordination. Moreover, with regard to Equation (2), we note a considerable elongation of the M–N bonds in the MN_3O_3 structures. This effect is most pronounced for Fe^{III} (compare the observed mean bond lengths Fe–O: 1.96, Fe–N: 2.18 Å with the calculated values Fe–O: 2.01, Fe–N: 2.08 Å, obtained from Eq. (1) and (2), respectively). The observed deviations of the M–N and M–O bond lengths from Equations (1) and (2) for the N_3O_3 coordination can be explained by a partial release of electron density from the deprotonated oxygen donors to the metal cation by bonding of a $p_\pi \rightarrow d_\pi$ type,[39] where complexes with a *trans*-O-M-O geometry are destabilized by increased antibonding interactions.[25] Experimental corroboration of this interpretation was provided by Mössbauer spectroscopy. The isomer shift $\delta_{\alpha\text{-Fe}}$ of $[Fe(tdci)_2]^{3+}$ was found to be 0.74 ± 0.03 mm s^{-1} for the crystalline solid and 0.75 ± 0.05 mm s^{-1} for the frozen solution. The usual range for mononuclear, octahedral complexes is $0.3 < \delta_{\alpha\text{-Fe}} < 0.6$ mm s^{-1} for high-spin Fe^{III} and $1.0 < \delta_{\alpha\text{-Fe}} < 1.5$ mm s^{-1} for high-spin Fe^{II}.[39] Thus, the high value of $[Fe(tdci)_2]^{3+}$ indicates a significantly increased shielding of the nucleus, which is obviously a consequence of the enlarged electron density in the t_{2g} orbitals of the metal cation. In contrast to $[Fe(tdci)_2]^{3+}$, the isomer shift of $[Fe(taci)_2]^{3+}$ is not abnormal.

$$d(M-N) = 1.44\ \text{Å} + r_M \qquad (2)$$

The Stability of Tdci Complexes with Different Metal Ions: The complexation of metal ions like Al^{3+}, Ti^{4+}, and Ge^{4+} with alkoxide ligands has been well known for many years, however, these complexes usually undergo rapid hydrolysis in aqueous solution and can therefore only be investigated in rigorously dried organic solvents.[41] The ligand tdci is quite unique with respect to its ability to bind a variety of trivalent and tetravalent metal ions exclusively through alkoxo groups and to form mononuclear complexes, which are stable in aqueous solution over a wide range of the pH scale (Fig. 2). The remarkable stability of tdci complexes is based on the very rigid structure of this ligand with three donor groups in an optimal position for metal binding. These geometric properties, which are responsible for a very high chelate effect, are combined with the presence of three equivalents of base within the molecule, which facilitate the required deprotonation of the hydroxyl groups. In fact, the formation of the zwitterionic form of tdci requires much less energy than the complete deprotonation. This is easily understandable, considering the fact that the zwitterionic form is still a neutral molecule, and additional electrostatic work is required to generate the completely deprotonated, trinegative anion. These considerations were confirmed experimentally by introducing three permanent positive charges on the nitrogen atoms; the resulting polyalcohol has an unusually low pK_a value of 8.1.[10]

Tdci must be considered as one of the most effective ligand known for small and hard trivalent and tetravalent metal ions. The observed formation constants for Al^{3+}, Fe^{3+}, and Ga^{3+} are very high. In fact, it has been shown that tdci easily competes with polyaminopolycarboxylates like NTA or EDTA at neutral pH.[9]

A comparison of the stability of the four trivalent metal ions is of particular interest. For Al^{3+}, Ga^{3+}, and Fe^{3+} linear free energy relations were postulated for oxygen-bound complexes, and the order of increasing stability $Al^{III} < Ga^{III} < Fe^{III}$ is well established.[42] Our results are in good agreement with these relations. Martell et al.[23] found an increase in stability in the order $Ga^{III} < In^{III}$ for a variety of polyaminopolycarboxylato complexes, whereas for the "harder" polyaminopolyphenolato ligands the reverse order was established. The significant decrease in stability for $[Ga(tdci)_2]^{3+} > [In(tdci)_2]^{3+}$ can thus be readily understood, since the metal ions of these two complexes are now exclusively bound to the "very hard" alkoxo ligands.

Comparison of Tdci and Taci Complexes in Aqueous Solution: The formation constants and pK_a values of taci and tdci complexes are summarized in Table 13. Comparing taci with tdci, we note two important characteristics: a) Metal ions with a preference for the O_6 coordination mode form significantly more stable complexes with tdci. Even for metal cations like Ga^{3+} and In^{3+}, where different coordination modes are observed for $[M(taci)_2]^{3+}$ and $[M(tdci)_2]^{3+}$, tdci is still a more effective ligand. Only Tl^{III}, which has a very high preference for nitrogen donors, forms a more stable complex with taci. The X-ray data of $[Al(taci)_2]^{3+}$ and $[Al(tdci)_2]^{3+}$ show, however, no significant structural differences for the coordination spheres of the two complexes.[4] Even the six water molecules, which are hydrogen bonded to the alkoxo groups and form a second coordination sphere, are arranged in the same way (Fig. 4). Thus, the remarkably increased stability of the tdci complexes can certainly not be explained by a different type of interaction between the donor atoms and the metal center. b) The peripheral, noncoordinating dimethylammonium groups of the bis complexes are weakly acidic and can be deprotonated in aqueous solution. The acidity constants are basically a function of the charge of the metal center. Replacement of the metal center by an other cation of the same charge does not result in a significant change of the pK_as, as expected for an electrostatic interaction. On the other hand, going from taci to tdci, a significant decrease in the pK_as is noted, particularly for metal complexes with trivalent cations. In the course of a progressive deprotonation, the difference in acidity between the taci and tdci complexes is even enlarged. It is too high to be explained exclusively by the increased basicity of the tertiary amine.

Table 13. Comparison of formation constants of corresponding taci [a] and tdci [b] complexes.

	$[Al(taci)_2]^{3+}$	$[Al(tdci)_2]^{3+}$	$[Ga(taci)_2]^{3+}$	$[Ga(tdci)_2]^{3+}$
$\log\beta_1$ [c]	11.8	14.3	16.5	16.6
$\log\beta_2$ [d]	18.8	26.3	25.7	30.3
pK_1 [e]	8.1	10.1	7.4	10.0

[a] From ref. [4]. [b] This work. [c] $\beta_1 = [M(tdci)][M]^{-1}[tdci]^{-1}$. [d] $\beta_2 = [M(tdci)_2][M]^{-1}[tdci]^{-2}$. [e] $pK_1 = -\log K_1$, $K_1 = [H_{-1}M(tdci)_2][H][M(tdci)_2]^{-1}$.

The reduced acidity of the peripheral ammonium groups in the tdci complexes can however be explained, if one assumes that a similar type of hydration is observed in aqueous solution as in the solid state (Figs. 4 and 5). The N–H protons of the tdci complexes are involved in a tight network of hydrogen bonds within the first and the second coordination sphere of the complex. Deprotonation causes a breakdown of this network and

0570-0833/95/0101-0086 $ 10.00+.25/0 Chem. Eur. J. 1995, 1, No. 1

therefore requires additional energy. According to the X-ray analysis, the same type of second coordination sphere is also observed for a corresponding taci complex; however, since three protons are attached to each nitrogen atom, deprotonation can now easily occur without destruction of the second coordination sphere.

It also seems possible that this particular type of hydration is responsible for the increased stability of tdci complexes. As noted above, the six dimethylammonium groups together with the two cyclohexane rings of a bis(tdci) complex shield the hydrophilic part of the complex and generate a lipophilic surface. Thus, after the hydrophilic pocket has been filled by water molecules, the entire $[(M(tdci)_2(H_2O)_6)(H_2O)_6]^{z+}$ entity must be regarded as a rather lipophilic species with only weak interactions to further solvent molecules. Therefore, structural effects on the bulk solvent are almost negligible. In contrast, a bis(taci) complex has a very hydrophilic surface, and the additional N–H protons will strongly interact with the bulk solvent. The different nature of the molecular surface is also demonstrated by the solid state structure (Fig. 5). In the crystal structure, no significant intermolecular interactions between adjacent $[(M(tdci)_2(H_2O)_6)]^{3+}$ units are observed, whereas the $[Al(taci)_2(H_2O)_6]^{3+}$ aggregates are connected by intermolecular hydrogen bonds, involving one of the additional N–H protons that does not participate in the intramolecular network of hydrogen bonds. It thus becomes clear that the tdci complex is probably stabilized owing to a favorable entropy of hydration ΔS. Of course, the stronger hydration of the taci complex causes a more favorable ΔH. However, this effect is not relevant for the complex formation since it is already present for the free ligands.

Conclusion

Comparison of Taci and Tdci: The replacement of the amino groups by dimethylamino groups has four major implications for the coordination properties of the two ligands:

a) The present study clearly confirmed the inability of tdci to coordinate a metal cation by three nitrogen donors. In all complexes presented in this report, tdci binds the metal ion exclusively through oxygen donors, even when a coordination through nitrogen donors is observed in the corresponding taci complex. The selectivity of tdci for oxophilic cations is illustrated by the observation that metal ions with a very high preference for nitrogen donors like Tl^{III} do not form any stable complexes with tdci in aqueous solution.

b) Owing to the well-known enhanced donor strength of the tertiary amino groups, tdci is a stronger base. The increased basicity of tdci is of importance even if the cation binds exclusively to the oxygen donors, since it facilitates the proton transfer from OH to N and thus stabilizes the zwitterionic form required for coordination.

c) The six additional methyl groups make tdci much more lipophilic. This effect is particularly pronounced in the bis complexes where the hydrophilic part is hidden in the inside of the complex molecule and is almost completely shielded by a hydrophobic surface formed by the twelve methyl groups. As a consequence, tdci complexes are soluble in organic solvents like MeOH, whereas the corresponding taci complexes are only soluble in water. Moreover, the weak interaction between the outside of the complex molecule and the bulk solvent results in a more favorable ΔS. This effect is probably responsible for the significant increase in stability of tdci complexes. Thus, the taci–tdci system is an illustrative model, which demonstrates that even peripheral alterations of the ligand geometry may result in dramatic, unexpected changes of the metal-binding properties.

d) The N–H groups in the $[M(tdci)_2]^{3+}$ complexes are involved in a tight network of hydrogen bonds. Removal of the N–H protons results in a breakdown of this network, and consequently rather high pK_a values were observed for the N–H groups in these complexes. A similar network is also formed in the corresponding taci complexes. However, since taci has additional N–H protons, which are not involved in hydrogen bonding of the second coordination sphere, a deprotonation of the complex can occur without rupture of this network. Indeed, the present work shows significantly lower pK_a values for corresponding taci complexes. Thus, the deprotonation of $[M(taci)_2]^{3+}$ at high pH is strongly exergonic and represents a significant stabilization of such species. Since this effect is much less pronounced for tdci, it might be possible to reverse the order of complexation ability tdci > taci observed in neutral and acidic solutions. There is thus evidence that in strongly alkaline solution, taci is a more efficient chelator than tdci for hard highly charged cations.

Acknowledgement: We thank Marc Meienberger and Beat Müller for the measurement of the NMR spectra and Rolf Häfliger for recording the FAB mass spectra. Financial support of this work by Kredite für Unterricht und Forschung, ETH Zürich, is gratefully acknowledged.

Supplementary Material Available: Further details of the crystal structure investigation are available on request from the Director of the Cambridge Crystallographic Data Centre, 12 Union Road, GB-Cambridge CB21EZ (UK), on quoting the full journal citation. The Figures S1 and S2, showing NMR spectra of $[M(tdci)_2]Cl_3$ (M = Ga, In) as a function of pD may be obtained from the correspondence author (K. H.).

Received: October 18, 1994 [F3]

[1] H. W. Schmalle, K. Hegetschweiler, M. Ghisletta, *Acta Crystallogr.* **1991**, *C47*, 2047.
[2] K. Hegetschweiler, V. Gramlich, M. Ghisletta, H. Samaras, *Inorg. Chem.* **1992**, *31*, 2341.
[3] M. Ghisletta, H.-P. Jalett, T. Gerfin, V. Gramlich, K. Hegetschweiler, *Helv. Chim. Acta* **1992**, *75*, 2233.
[4] K. Hegetschweiler, M. Ghisletta, T. F. Fässler, R. Nesper, H. W. Schmalle, G. Rihs, *Inorg. Chem.* **1993**, *32*, 2032.
[5] K. Hegetschweiler, M. Ghisletta, V. Gramlich, *Inorg. Chem.* **1993**, *32*, 2699.
[6] K. Hegetschweiler, R. D. Hancock, M. Ghisletta, T. Kradolfer, V. Gramlich, H. W. Schmalle, *Inorg. Chem.* **1993**, *32*, 5273.
[7] K. Hegetschweiler, M. Ghisletta, T. F. Fässler, R. Nesper, *Angew. Chem. Int. Ed. Engl.* **1993**, *32*, 1426.
[8] K. Hegetschweiler, A. Egli, R. Alberto, H. W. Schmalle, *Inorg. Chem.* **1992**, *31*, 4027.
[9] T. Kradolfer, K. Hegetschweiler, *Helv. Chim. Acta* **1992**, *75*, 2243.
[10] K. Hegetschweiler, I. Erni, W. Schneider, H. Schmalle, *Helv. Chim. Acta* **1990**, *73*, 97.
[11] a) R. C. Hider, A. D. Hall, *Prog. Med. Chem.* **1991**, *28*, 40–173. b) R. C. Hider, S. Singh, J. B. Porter, *Proc. R. Soc. Edingburgh* **1992**, *99B*, 137–168.
[12] R. C. Weast, *Handbook of Chemistry and Physics*; 58th ed., CRC Press, Ohio, **1977**.
[13] M. D. Meienberger, K. Hegetschweiler, H. Rüegger, V. Gramlich; *Inorg. Chim. Acta* **1993**, *213*, 157.
[14] H. E. Baumgarten, J. M. Petersen, *Org. Syn.* **1961**, *41*, 82.
[15] The elemental analyses of several solid tdci metal complexes with a high amount of water of crystallization showed a H content that was generally too low. The same result was found previously for the Al and Fe complexes of tdci [9], indicating a systematic error for the determination of H in such compounds.
[16] G. M. Sheldrick, *SHELXTL-PLUS 88. Structure Determination Software Programs*; Nicolet Instrument Corp., Madison, WI, **1988**.
[17] SYBYL Program, available from TRIPOS Associates, **1699** South Hanley Road, St. Louis, MO 63144.
[18] R. D. Hancock, K. Hegetschweiler, *J. Chem. Soc., Dalton Trans.* **1993**, 2137.
[19] B. P. Hay, J. R. Rustad, C. J. Hostetler, *J. Am. Chem. Soc.* **1993**, *115*, 11158.
[20] P. Gans, A. Sabatini, A. Vacca, *J. Chem. Soc. Dalton Trans.* **1985**, 1195.
[21] R. J. Motekaitis, A. E. Martell, *Can. J. Chem.* **1982**, *60*, 2403.
[22] $\sigma_{pH} = (\sum w(pH_{obs} - pH_{calcd})^2/\sum w)^{1/2}$, $w = (pH_{i+1} - pH_{i-1})^{-2}$

[23] R. Delgado, Y. Sun, R. J. Motekaitis, A. E. Martell, *Inorg. Chem.* **1993**, *32*, 3320.
[24] C. F. Baes, R. E. Mesmer, *The Hydrolysis of Cations*; Wiley, New York, **1976**, p. 320.
[25] K. Hegetschweiler, M. Ghisletta, L. Hausherr-Primo, T. Kradolfer, H. W. Schmalle, V. Gramlich, *Inorg. Chem.* **1995**, in press.
[26] Intraligand angles are indicated as O-M-O, interligand angles as O-M-O'.
[27] An average Al–O bond length of 1.89 Å was calculated from a total of 38 mononuclear complexes with an AlO_6 coordination using the Cambridge Structural Database (see F. H. Allen, J. E. Davies, J. J. Galloy, O. Johnson, O. Kennard, C. F. Macrae, E. M. Mitchell, G. F. Mitchell, J. M. Smith, D. G. Watson, *J. Chem. Info. Comp. Sci.* **1991**, *31*, 187).
[28] An average Fe–O bond length of 2.01 Å was calculated from a total of 73 mononuclear complexes with an FeO_6 coordination using the Cambridge Structural Database (see ref. [27]).
[29] An average Ga–O bond length of 1.97 Å was calculated from a total of 14 mononuclear complexes with a GaO_6 coordination using the Cambridge Structural Database (see ref. [27]).
[30] An average In–O bond length of 2.14 Å was calculated from a total of 6 mononuclear complexes with an InO_6 coordination using the Cambridge Structural Database (see ref. [27]).
[31] a) Y. Zhang, R. A. Cedergren, T. J. Nieuwenhuis, R. I. Hollingsworth, *Anal. Biochem.* **1993**, *208*, 363. b) G. J. C. Paul, S. Bourg, M. J. Bertrand, *J. Am. Soc. Mass Spectrom.* **1993**, *4*, 493.
[32] The characteristic absorption peaks of tdci in the fingerprint region ($1500\,cm^{-1}$ to $1000\,cm^{-1}$) were not present in the spectrum and an intense absorption peak at $466\,cm^{-1}$ was attributed to the Ga–O vibration.
[33] R. J. Motekaitis, A. E. Martell, *Inorg. Chem.* **1980**, *19*, 1646.
[34] G. Anderegg, E. Hubmann, N. G. Podder, F. Wenk, *Helv. Chim. Acta* **1977**, *60*, 123.
[35] a) R. Benn, A. Rufinska, E. Janssen, H. Lehmkuhl, *Organometallics* **1986**, *5*, 825 827. b) M. R. P. van Vliet, P. Buysingh, G. van Koten, K. Vrieze, B. Kojic-Prodic, A. L. Spek, *Organometallics* **1985**, *4*, 1701.
[36] R. D. Shannon, *Acta Crystallogr.* **1976**, *A32*, 751.
[37] M. C. Ghisletta, Dissertation No. 10891, ETH-Zürich, Switzerland, **1994**.
[38] For most metal ions, $\log K_1(M-NH_3)$ is known experimentally (see A. E. Martell, R. M. Smith, *Critical Stability Constants*, Plenum Press, New York, **1974–1989**; Vols 1–6), the others were calculated (see F. Mulla, F. Marsicano, B. S. Nakani, R. D. Hancock, *Inorg. Chem.* **1985**, *24*, 3076; and R. D. Hancock, A. E. Martell, *Chem. Rev.* **1989**, *89*, 1875).
[39] U. Auerbach, T. Weyhermüller, K. Wieghardt, B. Nuber, E. Bill, C. Butzlaff, A. X. Trautwein, *Inorg. Chem.* **1993**, *32*, 508.
[40] Addition of $In(NO_3)_3$ (1 equiv, dissolved in MeOH) to a methanolic solution of taci (2 equiv) resulted in a crude product containing predominantly mononuclear $[In(taci)_2]^{3+}$ (see ref. [7]). FAB^+-MS: *m/z* 467.1 ($[In(taci)_2-2H]^+$). ^1H NMR: $\delta = 3.79, 4.08$; ^{13}C NMR: $\delta = 67.4, 59.8$. According to refs. [4], [6], and [13], the NMR data clearly indicate the presence of a bis-type(i) structure.
[41] a) D. C. Bradley, R. C. Mehrotra, D. P. Gaur, Metal Alkoxides, Academic Press, London, **1978**. b) K. G. Caulton, L. G. Hubert-Pfalzgraf, *Chem. Rev.* **1990**, *90*, 969–995.
[42] $\log K_{GaL} = 0.8 + 0.86 \log K_{FeL}$, $\log K_{AlL} = 0.3 + 0.71 \log K_{FeL}$; see R. B. Martin, *Met. Ions Biol. Syst.* **1988**, *24*, 1. Compare the experimental value $\log K_{GaL} = 16.6$ and $\log K_{AlL} = 14.3$ with 17.0 (Ga) and 13.7 (Al) calculated accordingly from $\log K_{FeL} = 18.8$.
[43] In this work the terms alkalimetric and acidimetric titration refer to the addition to the test solution of base and acid, respectively.

0570-0833/95/0101-0088 $ 10.00+.25/0